Appendix A.26:

Ti Rakau Reserve – VsVp 57186

Table 1: Site Description for Ti Rakau Reserve (VsVp 57186).

Attribute	Yes/No			Description/Date	Symbol in Figure 1
	10-m Buffer	20-m Buffer	50-m Buffer		
Near a body of surface water or other free face features?	No	No	No	The center of the site is ~190 m away from the channel that runs in the NW-SE direction. The nearby bodies of surface water are also the Steamwharf Stream (~470 m away) to the SW, the Heathcote River (~660 m away) to the S, and Avon Heathcote Estuary (~690 m away) to the E. The height of the nearest free face is ~1.5 m.	NA
Lateral spreading observed during the CES?	No	No	No	No lateral spreading was observed by the mapping team.[1]	NA
Nearby buildings or structures?	No	No	Yes	Building coverage of the 50-m buffer is 12%.	White Fill + Brown Outline
Sloping land?	No	No	No	Flat land, open + residential area	NA
Step changes in the ground surface?	No	No	No	NA	NA
Retaining walls?	No	No	No	NA	NA
Vegetation?	Yes	Yes	Yes	Trees and bushes cover 3, 31, and 19% of the 10-, 20-, and 50-m buffer, respectively. They are in all quadrants of the 20- and 50-m buffers and the NE quadrant only of the 10-m buffer.	White Fill + Green Outline
Anthropogenic changes to the site between the LiDAR surveys?	Yes	Yes	Yes	House construction in the SW quadrant of the 50-m buffer between Jan 2003 and Dec 2004. Landscaping in the E portion of the 50-m buffer between Oct 2009 and Sep 2010. House removal in the NE quadrant of the 50-m buffer between Mar and Aug 2013. House reconstruction in the SE quadrant of the 50-m buffer between Mar and Aug 2014. Minor earthwork (possible re-grassing) in all quadrants of all buffers between Jul 2015 and Jan 2015.	Building Addition/Demolition: Orange Crossline
Other important factors?	No	Yes	Yes	Ti Rakau Dr in the NW and SW quadrants and Kestrel Pl in the NW and NE quadrants occupy 15% of the 50-m buffer. Ti Rakau Dr covers only 1% of the 20-m buffer in the NW quadrant. Playground is in the SE quadrant of the 50-m buffer. Three ditches in the E portion of the 50-m buffer. Two lamp posts are in the NW and SW quadrants of the 50-m buffer. Two mounds are in the SE quadrant of the 50-m buffer.	Playground: White Fill + Orange Outline; Ti Rakau Dr and Kestrel Pl: Gray Fill + Red Outline; Ditch: White Fill + Purple Outline; Lamp Post: White Fill + Cyan Outline; Mounds: White Fill + Yellow Outline

Note: Buffer is the area within a circle of a specified radius with CPT investigations done at its center (172.695373°, -43.548825°).

[1] Canterbury Geotechnical Database. (2012). "Observed Ground Crack Locations", Map Layer CGD0400 - 23 July 2012, retrieved July 09, 2018 from https://canterburygeotechnicaldatabase.projectorbit.com/

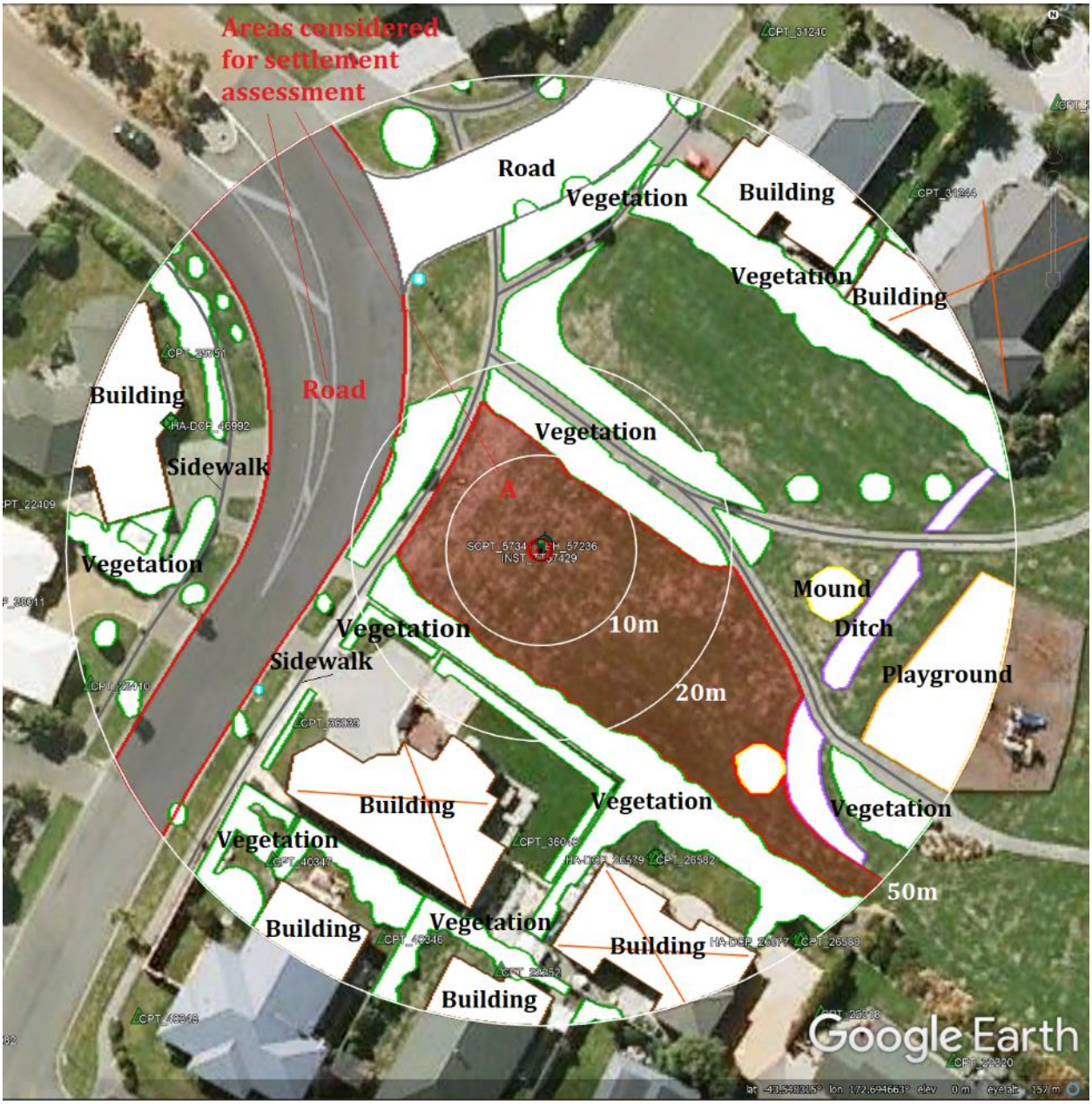

Figure 1: Site plan with areas where ejecta-induced settlement data is considered.

Note 1: Patch A (outlined in red) in the free field was selected for settlement assessment as an area free of vegetation and structures. Other important factors considered in the patch selection process were its proximity to a CPT, a property subjected to addition and/or demolition of a structure, front yard/backyard alterations (e.g., ploughing, rubble, scrap), and aerial distribution of sediment ejecta. In addition, since significant amounts of ejecta were observed on roads in the CES, the entire portion of the road within the 50-m buffer was considered for settlement assessment. The LiDAR surveys were available for the Jun-11 and Dec-11 EQs only; however, they were not used to estimate the ejecta-induced settlement.

Table 2: LiDAR flight error adjustments, global adjustments for the difference between average LiDAR point elevations and benchmark survey elevations, and vertical tectonic movement adjustments.

	Adjustments (mm)		
Earthquake Event(s)	LiDAR Flight Error	Global Offset[2]	Tectonic Vertical Movement
Sep-10	NA	-3	0
Feb-11	NA	16	+350
Jun-11	0	38	-25
Dec-11	-100	-65	+25
CES	-100	-14	+350
Any LiDAR survey affected by ejecta?			No

Notes: The negative sign indicates the subtraction from the ground surface subsidence, while the positive sign indicates the addition to the ground surface subsidence; NA = Not available because the Sep-2010 LiDAR survey did not cover the site.

Table 3a: LiDAR Measurement Error for Patch A.

Surveys	Buffer	Area Averaged Difference Indicating Repeat Measurement Error (mm)	$\sigma^*_{\text{individual LiDAR points}}$ (mm)	%Reduction in σ due to Area Averaging of LiDAR Points
Post Feb 2011: Mar 2011 and May 2011	10-m	ND	59	[ND,ND]
	20-m	ND		
	50-m	ND		
Post Dec 2011: Feb 2012 and Oct 2015	10-m	ND	70	[ND,ND]
	20-m	ND		
	50-m	ND		

*Standard deviation.

[2] Russell, J., & van Ballegooy, S. (2015). *Canterbury Earthquake Sequence: Increased liquefaction vulnerability assessment methodology*. New Zealand: Tonkin & Taylor Ltd.

Table 3b: LiDAR Measurement Error for Road.

Surveys	Buffer	Area Averaged Difference Indicating Repeat Measurement Error (mm)	$\sigma^*_{\text{individual LiDAR points}}$ (mm)	%Reduction in σ due to Area Averaging of LiDAR Points
Post Feb 2011: Mar 2011 and May 2011	10-m	NA	59	[ND,ND]
	20-m	ND		
	50-m	ND		
Post Dec 2011: Feb 2012 and Oct 2015	10-m	NA	70	[ND,ND]
	20-m	ND		
	50-m	ND		

*Standard deviation.

Table 4a: Ground surface subsidence adjustments due to LiDAR measurement error for Patch A.

Earthquake Event(s)	$\sigma_{\text{pre-EQ LiDAR survey}}$ (mm)	$\sigma_{\text{post-EQ LiDAR survey}}$ (mm)	σ_{total} (mm)	Area Average Adjusted σ (mm) **
Sep-10	158	56	134	±ND
Feb-11	56	59	59	±ND
Jun-11	59	61	62	±ND
Dec-11	61	70	87	±ND
CES	158	70	124	±ND

**Based on the highest %Reduction in Table 3.

Table 4b: Ground surface subsidence adjustments due to LiDAR measurement error for Road.

Earthquake Event(s)	$\sigma_{\text{pre-EQ LiDAR survey}}$ (mm)	$\sigma_{\text{post-EQ LiDAR survey}}$ (mm)	σ_{total} (mm)	Area Average Adjusted σ (mm) **
Sep-10	158	56	134	±ND
Feb-11	56	59	59	±ND
Jun-11	59	61	62	±ND
Dec-11	61	70	87	±ND
CES	158	70	124	±ND

**Based on the highest %Reduction in Table 3.

Table 5a: Raw liquefaction-related ground surface subsidence using original LiDAR points for Patch A.

	Average Ground Surface Subsidence (mm)		
Earthquake Event(s)	10-m Buffer	20-m Buffer	50-m Buffer
Sep-10	NA	NA	NA
Feb-11	NA	NA	NA
Jun-11	ND	ND	ND
Dec-11	ND	ND	ND
CES	ND	ND	ND

Note: NA = Not available; ND = Not determined.

Table 5b: Raw liquefaction-related ground surface subsidence using original LiDAR points for Road.

	Average Ground Surface Subsidence (mm)		
Earthquake Event(s)	10-m Buffer	20-m Buffer	50-m Buffer
Sep-10	NA	NA	NA
Feb-11	NA	NA	NA
Jun-11	NA	ND	ND
Dec-11	NA	ND	ND
CES	NA	ND	ND

Note: NA = Not available; ND = Not determined.

Table 6a: Corrected liquefaction-related ground surface subsidence using original LiDAR points for Patch A with the calculated adjustments in Table 2.

	Average Calculated Ground Surface Subsidence (mm)		
Earthquake Event(s)	10-m Buffer	20-m Buffer	50-m Buffer
Sep-10	NA	NA	NA
Feb-11	NA	NA	NA
Jun-11	ND	ND	ND
Dec-11	ND	ND	ND
CES	ND	ND	ND

Notes: Plus/minus values are same as those in Table 4, but rounded to the nearest 25 mm; Positive overall values indicate ground surface subsidence, while negative overall values indicate ground surface uplift; NA = Not available; ND = Not determined.

Table 6b: Corrected liquefaction-related ground surface subsidence using original LiDAR points for Road with the calculated adjustments in Table 2.

	Average Calculated Ground Surface Subsidence (mm)		
Earthquake Event(s)	10-m Buffer	20-m Buffer	50-m Buffer
Sep-10	NA	NA	NA
Feb-11	NA	NA	NA
Jun-11	NA	ND	ND
Dec-11	NA	ND	ND
CES	NA	ND	ND

Notes: Plus/minus values are same as those in Table 4, but rounded to the nearest 25 mm; Positive overall values indicate ground surface subsidence, while negative overall values indicate ground surface uplift; NA = Not available; ND = Not determined.

Table 7a: Corrected liquefaction-related ground surface subsidence for Patch A using LiDAR DEMs.

	Estimated Ground Surface Subsidence (mm)								
	10-m Buffer			20-m Buffer			50-m Buffer		
Earthquake Event(s)	16th %ile	50th %ile	84th %ile	16th %ile	50th %ile	84th %ile	16th %ile	50th %ile	84th %ile
Sep-10	NA	NA	NA	NA	NA	NA	NA	NA	NA
Feb-11	NA	NA	NA	NA	NA	NA	NA	NA	NA
Jun-11	<50	50	50	<50	50	50	<50	50	50
Dec-11	<50	50	50	<50	50	50	<50	50	50
CES	<50	<50	<50	<50	<50	<50	<50	<50	50

Note: These percentiles are not the exact statistical measures; they indicate the spatial variability of ground surface subsidence.

Table 7b: Corrected liquefaction-related ground surface subsidence for Road using LiDAR DEMs.

	Estimated Ground Surface Subsidence (mm)								
	10-m Buffer			20-m Buffer			50-m Buffer		
Earthquake Event(s)	16th %ile	50th %ile	84th %ile	16th %ile	50th %ile	84th %ile	16th %ile	50th %ile	84th %ile
Sep-10	NA	NA	NA	NA	NA	NA	NA	NA	NA
Feb-11	NA	NA	NA	NA	NA	NA	NA	NA	NA
Jun-11	NA	NA	NA	ND	ND	ND	<50	50	50
Dec-11	NA	NA	NA	ND	ND	ND	<50	<50	50
CES	NA	NA	NA	ND	ND	ND	<50	50	50

Note: These percentiles are not the exact statistical measures; they indicate the spatial variability of ground surface subsidence.

Table 8a: Ejecta-Induced settlement for the top 20 m of the soil profile for Patch A (10-m and 20-m buffers) for the 50th %ile PGA, P_L=50%, and C_{FC}=0.13 using BI-2014, ZRB-2002, and I_c cutoff of 2.6.

Earthquake Event(s)	M_W	PGA (g)	Depth to Groundwater (m)	S_T (mm)	S_{V1D} (mm)	$S_{E,L}$ (mm)
Sep-10	7.1	0.23	0.5	NA	34±20	NA
Feb-11	6.2	0.68	0.5	NA	176±50	NA
Jun-11	6.2	0.43	0.5	ND	99±25	ND
Dec-11	6.1	0.30	1.1	ND	22±50	ND

Notes: S_T = Total settlement (Table 6); S_{V1D} = Average vertical settlement due to volumetric compression using Boulanger and Idriss (2014) (BI-2014), Zhang et al. (2002) (ZRB-2002) procedures and de Greef and Lengkeek (2018) thin-layer correction; $S_{E,L}$ = Ejecta-induced settlement as the difference between the LiDAR-based S_T and S_{V1D}; NA = Not available due to the absence of the Sep-2010 LiDAR survey from the site.

Table 8b: Ejecta-Induced settlement for the top 20 m of the soil profile for Patch A (50-m buffer) for the 50th %ile PGA, P_L=50%, and C_{FC}=0.13 using BI-2014, ZRB-2002, and I_c cutoff of 2.6.

Earthquake Event(s)	M_W	PGA (g)	Depth to Groundwater (m)	S_T (mm)	S_{V1D} (mm)	$S_{E,L}$ (mm)
Sep-10	7.1	0.23	0.5	NA	65±20	NA
Feb-11	6.2	0.68	0.5	NA	183±50	NA
Jun-11	6.2	0.43	0.5	ND	127±25	ND
Dec-11	6.1	0.30	1.1	ND	54±50	ND

Notes: S_T = Total settlement (Table 6); S_{V1D} = Average vertical settlement due to volumetric compression using Boulanger and Idriss (2014) (BI-2014), Zhang et al. (2002) (ZRB-2002) procedures and de Greef and Lengkeek (2018) thin-layer correction; $S_{E,L}$ = Ejecta-induced settlement as the difference between the LiDAR-based S_T and S_{V1D}; NA = Not available due to the absence of the Sep-2010 LiDAR survey from the site.

Table 8c: Ejecta-Induced settlement for the top 20 m of the soil profile for Road (50-m buffer) for the 50th %ile PGA, P_L=50%, and C_{FC}=0.13 using BI-2014, ZRB-2002, and I_c cutoff of 2.6.

Earthquake Event(s)	M_W	PGA (g)	Depth to Groundwater (m)	S_T (mm)	S_{V1D} (mm)	$S_{E,L}$ (mm)
Sep-10	7.1	0.23	0.5	NA	94±20	NA
Feb-11	6.2	0.68	0.5	NA	211±50	NA
Jun-11	6.2	0.43	0.5	ND	158±25	ND
Dec-11	6.1	0.30	1.1	ND	81±50	ND

Notes: S_T = Total settlement (Table 6); S_{V1D} = Average vertical settlement due to volumetric compression using Boulanger and Idriss (2014) (BI-2014), Zhang et al. (2002) (ZRB-2002) procedures and de Greef and Lengkeek (2018) thin-layer correction; $S_{E,L}$ = Ejecta-induced settlement as the difference between the LiDAR-based S_T and S_{V1D}; NA = Not available due to the absence of the Sep-2010 LiDAR survey from the site.

Note 3: The uncertainty for volumetric settlement was derived based on the sensitivity of volumetric settlement to PGA, C_{FC}, and P_L for each earthquake event for VsVp 57203 *Shirley Intermediate School* and CC LIQ 1 – CPT 5586 – *Vivian St* sites. Taking the 50th percentile as the baseline case, the minimum and maximum values corresponding to the difference between the 25th percentile and the 50th percentile and the 75th percentile and the 50th percentile were determined. The arithmetic mean of the range of the minimum and maximum difference was evaluated for each patch at the two sites. The maximum arithmetic mean for each earthquake event was rounded to the nearest five and used as the uncertainty value. Accordingly, the 1-D volumetric settlement uncertainties of ±20, ±50, ±25, and ±50 mm for the Sep-10, Feb-11, Jun-11, and Dec-11 earthquake events, respectively, were used for all sites in this study.

Table 9a: Coverage area and height of ejecta estimates for Patch A (10-m buffer) using photographs.

EQ Event	$H_{E,thick1}$ (mm)	$A_{E,thick1}$ (m^2)	$H_{E,thick2}$ (mm)	$A_{E,thick2}$ (m^2)	$H_{E,thin}$ (mm)	$A_{E,thin}$ (m^2)	A_T (m^2)
Sep-10	0	0	0	0	0	0	306
Feb-11	100-180	55.5	0	0	5-10	8.9	306
Jun-11	60-120	36.4	40-80	34.1	0	0	306
Dec-11	0	0	20-40	6.0	0	0	306

Notes: $A_{E,thin/thick}$ = Coverage area of thin ejecta layers; $H_{E,thin/thick}$ = Lower-upper estimate of height of thin/thick ejecta layers; A_T= Total assessment area of a buffer being considered.

Table 9b: Coverage area and height of ejecta estimates for Patch A (20-m buffer) using photographs.

EQ Event	$H_{E,thick1}$ (mm)	$A_{E,thick1}$ (m^2)	$H_{E,thick2}$ (mm)	$A_{E,thick2}$ (m^2)	$H_{E,thin}$ (mm)	$A_{E,thin}$ (m^2)	A_T (m^2)
Sep-10	0	0	0	0	0	0	642
Feb-11	100-180	55.5	70-150	38.3	5-10	42.8	642
Jun-11	60-120	54.3	40-80	43.0	10-20	14.6	642
Dec-11	0	0	20-40	6.8	10-30	17.3	642

Notes: $A_{E,thin/thick}$ = Coverage area of thin ejecta layers; $H_{E,thin/thick}$ = Lower-upper estimate of height of thin/thick ejecta layers; A_T= Total assessment area of a buffer being considered.

Table 9c: Coverage area and height of ejecta estimates for Patch A (50-m buffer) using photographs.

EQ Event	$H_{E,thick1}$ (mm)	$A_{E,thick1}$ (m^2)	$H_{E,thick2}$ (mm)	$A_{E,thick2}$ (m^2)	$H_{E,thin}$ (mm)	$A_{E,thin1}$ (m^2)	A_T (m^2)
Sep-10	0	0	0	0	0	0	913
Feb-11	100-180	78.4	70-150	88.7	5-10	94.3	913
Jun-11	60-120	112.3	40-80	54.9	10-20	27.4	913
Dec-11	40-60	7.6	20-40	12.4	10-30	35.2	913

Notes: $A_{E,thin/thick}$ = Coverage area of thin ejecta layers; $H_{E,thin/thick}$ = Lower-upper estimate of height of thin/thick ejecta layers; A_T= Total assessment area of a buffer being considered.

Table 9d: Coverage area and height of ejecta estimates for Road (50-m buffer) using photographs.

EQ Event	$H_{E,trap.\ prism1}$ (mm)	$H_{E,trap.\ prism2}$ (mm)	$V_{E,trap.prism}$ (m^3)	$H_{E,prism/\ pyr}$ (mm)	$V_{E,prism+pyr}$ (m^3)	$H_{E,thick}$ (mm) $H_{E,cc}$ (mm)	$A_{E,thick}$ (m^2) $V_{E,cc}$ (m^3)	$H_{E,thin}$ (mm)	$A_{E,thin}$ (m^2)	A_T (m^2)
Sep-10	0	0	0	0	0	0	0	0	0	914
Feb-11	94-300	20-40	67.1-86.7	98-300	6.90-9.29	20-40	163	10-20	46.6	914
Jun-11	89-300	20-30	62.1-76.9	160-200	0.99-1.11	20-30	230	0	0	914
Dec-11	0	0	0	5-75	0.93-1.86	10-20 231-398	201 0.74	5-10	32.4	914

Notes: $H_{E,trap.\ prism1/2}$ = Lower-upper estimate of ejecta height at the curb/centerline based on 2-4% cross slope of normal crown and the maximum curb height of 150 mm; $V_{E,trap.\ prism}$ = Lower-upper estimate of total volume of ejecta shaped as a trapezoidal prism; $H_{E,prism/pyr}$ = Lower-upper estimate of ejecta height near the curb based on 2-4% cross slope of normal crown; $V_{E,prism+pyr}$ = Lower-upper estimate of total volume of prismatic- and pyramidal-shape ejecta; $A_{E,thin/thick}$ = Coverage area of thin/thick ejecta layers; $H_{E,thin/thick}$ = Lower-upper estimate of height of thin/thick ejecta layers; $H_{E,cc}$ = Lower-upper estimate of conically shaped ejecta pile component for the Dec-11 EQ; $V_{E,cc}$ = Total volume of conically shaped ejecta pile components for the Dec-11 EQ; A_T= Total assessment area of a buffer being considered.

Note 4: The values in Table 9 correspond to the coverage area of ejecta outlined in aerial photographs (Figures 10, 11, 13, 25, and 41-43) and the lower and upper estimates of ejecta height based on geometrical approximations, ground photographs (Figure 47), and EQC LDAT property inspection reports (e.g., Figures 44-46). The ejecta-induced settlement using photographs and engineering judgment, $S_{E,P}$, is estimated as

$$S_{E,P} = \frac{\sum_{i=1}^{a} A_{E,thick,i} * H_{E,thick,i} + \sum_{j=1}^{b} A_{E,thin,j} * H_{E,thin,j} + \frac{1}{3}\sum_{k=1}^{c} A_{E,pile,k} * R_{E,pile,k} * tan30°}{A_T}$$
$$+ \frac{\sum_{l=1}^{d} \left(\frac{1}{2}(H_{E,trap.\ prism\ 1,l} + H_{E,trap.\ prism\ 2,l}) * W_{E,trap.\ prism,l}\right) * L_{E,trap.\ prism,l}}{A_T}$$
$$+ \frac{\frac{1}{2}\sum_{n=1}^{f} W_{E,prism,n} * H_{E,prism,n} * L_{E,prism,n}}{A_T}$$
$$+ \frac{\frac{1}{3}\sum_{p=1}^{g} W_{E,r.pyramid,p} * H_{E,r.pyramid,p} * L_{E,r.pyramid,p}}{A_T}$$
$$+ \frac{\frac{1}{6}\sum_{r=1}^{h} W_{E,t.pyramid,r} * H_{E,t.pyramid,r} * L_{E,t.pyramid,r}}{A_T}$$
$$= \frac{\sum_{i=1}^{a} V_{E,thick,i} + \sum_{j=1}^{b} V_{E,thin,j} + \sum_{k=1}^{c} V_{E,conical\ component,k} + \sum_{l=1}^{d} V_{E,trap.\ prism,l}}{A_T}$$
$$+ \frac{\sum_{n=1}^{f} V_{E,prism,n} + \sum_{p=1}^{g} V_{E,r.pyramid,p} + \sum_{r=1}^{h} V_{E,t.pyramid,r}}{A_T}$$

where

- $A_{E,thick,i}$ and $H_{E,thick,i}$ are the area and the height, respectively, of a thick ejecta layer;
- $A_{E,thin,j}$ and $H_{E,thin,j}$ are the area and the height, respectively, of a thin ejecta layer;
- $A_{E,pile,k}$ and $R_{E,pile,k}$ are the area and the radius, respectively, of an ejecta pile component, shaped as a cone with the repose angle of 30°;
- $W_{E,trap.\ prism,l}$ and $L_{E,trap.\ prism,l}$ are the width and the length, respectively, of the coverage area of an ejecta layer shaped as a trapesoidal prism, while $H_{E,trap.\ prism\ 1,l}$ and $H_{E,trap.\ prism\ 2,l}$ are the heights of the trapesoidal prism-like ejecta layer;
- $W_{E,prism,n}$ and $L_{E,prism,n}$ are the width and the length, respectively, of the coverage area of a prismatically shaped ejecta layer, and $H_{E,prism,n}$ is the height of a prism-like ejecta layer;
- $W_{E,pyr,p}$ and $L_{E,pyr,p}$ are the width and the length, respectively, of the coverage area of a rectangular-base pyramid-like ejecta layer, and $H_{E,pyr,p}$ is the height of a pyramid-like ejecta layer;
- $W_{E,pyr,r}$ and $L_{E,pyr,r}$ are the width and the length, respectively, of the coverage area of a triangular-base pyramid-like ejecta layer, and $H_{E,pyr,r}$ is the height of a triangular-base pyramid-like ejecta layer;
- A_T is the total assessment area for a buffer being considered (Figure 1).

Table 10a: Ejecta-induced settlement estimates for Patch A based on photographs.

Earthquake Event	Patch A (10-m buffer)		Patch A (20-m buffer)		Patch A (50-m buffer)	
	$S_{E,P,lower}$ (mm)	$S_{E,P,upper}$ (mm)	$S_{E,P,lower}$ (mm)	$S_{E,P,upper}$ (mm)	$S_{E,P,lower}$ (mm)	$S_{E,P,upper}$ (mm)
Sep-10	0	0	0	0	0	0
Feb-11	18	33	13	25	16	31
Jun-11	12	23	8	16	10	20
Dec-11	≈0	1	≈0	1	1	2

Note: $S_{E,P,lower}$ and $S_{E,P,upper}$ correspond to lower and upper estimates of $S_{E,P}$, respectively.

Table 10b: Ejecta-induced settlement estimates for Road based on photographs.

Earthquake Event	Road (50-m buffer)	
	$S_{E,P,lower}$ (mm)	$S_{E,P,upper}$ (mm)
Sep-10	0	0
Feb-11	85	113
Jun-11	74	93
Dec-11	4	8

Note: $S_{E,P,lower}$ and $S_{E,P,upper}$ correspond to lower and upper estimates of $S_{E,P}$, respectively.

Table 11a: Best final estimates of ejecta-induced settlement for Patch A.

EQ Event	Patch A (10-m buffer)			Patch A (20-m buffer)			Patch A (50-m buffer)		
	$S_{E,L}$ (mm)	$S_{E,P}$ (mm)	$S_{E,final}$ (mm)	$S_{E,L}$ (mm)	$S_{E,P}$ (mm)	$S_{E,final}$ (mm)	$S_{E,L}$ (mm)	$S_{E,P}$ (mm)	$S_{E,final}$ (mm)
Sep-10	NA	0	0	NA	0	0	NA	0	0
Feb-11	NA	26±7	25±5	NA	19±6	20±5	NA	24±7	25±5
Jun-11	ND	18±5	20±5	ND	12±4	10±5	ND	15±5	15±5
Dec-11	ND	0.5±0.5	<5	ND	0.5±0.5	<5	ND	1.5±0.5	<5

Notes: $S_{E,L}$ = Ejecta-induced settlement based on LiDAR data reported in Table 8; $S_{E,P}$ = Median ejecta-induced settlement for the range of values reported in Table 10; $S_{E,final}$ = Best final estimate of ejecta-induced settlement rounded to the nearest 5 mm; Final plus/minus values are also rounded to the nearest 5 mm.

Table 11b: Best final estimates of ejecta-induced settlement for Road.

EQ Event	Road (50-m buffer)		
	$S_{E,L}$ (mm)	$S_{E,P}$ (mm)	$S_{E,final}$ (mm)
Sep-10	NA	0	0
Feb-11	NA	99±14	100±15
Jun-11	ND	84±9	85±10
Dec-11	ND	6±2	5±5

Notes: $S_{E,L}$ = Ejecta-induced settlement based on LiDAR data reported in Table 8; $S_{E,P}$ = Median ejecta-induced settlement for the range of values reported in Table 10; $S_{E,final}$ = Best final estimate of ejecta-induced settlement rounded to the nearest 5 mm; Final plus/minus values are also rounded to the nearest 5 mm.

Note 5:

- $S_{E,final}$ is based solely on $S_{E,P}$ for all earthquake events.
- The weight coefficients are based on the LiDAR error bands, LPI prediction error presence of The site is in the zone of accurate LPI prediction of liquefaction severity for the Sep-10 and slight to moderate LPI overprediction of liquefaction severity for the Feb-11 EQ (Maurer et al. 2014[3]). The LDAT inspection reports and ground photographs from Nov 2011 are available for the properties in the SE portion of the 50-m buffer. The height of ejecta at the time of the inspection was reported in the range from 50 mm to 300 mm. The inspection report and ground photographs for the property at the center of the site (Ti Rakau Reserve) are not available.

Summary 1:

- **The best estimate of the ejecta-induced free-field ground settlement at the Ti Rakau Reserve site for the SEP 2010, FEB 2011, JUN 2011, and DEC 2011 earthquake is 0 mm, 25±5 mm, 20±5 mm, and <5 mm, respectively.**
- **The best estimate of the ejecta-induced settlement of the road at the Ti Rakau Reserve site for the SEP 2010, FEB 2011, JUN 2011, and DEC 2011 earthquake is 0 mm, 100±15 mm, 85±10 mm, and 5±5 mm, respectively.**
- **The ejecta-induced settlement of the road is more representative of the site.**

[3] Maurer, B. W., Green, R. A., Cubrinovski, M., & Bradley, B. A. (2014). Evaluation of the Liquefaction Potential Index for Assessing Liquefaction Hazard in Christchurch, New Zealand. *Journal of Geotechnical and Geoenvironmental Engineering*, 140(7), 04014032-1-11. doi:10.1061/(asce)gt.1943-5606.0001117

Figure 2: Location of the site.

Figure 3: Position of the site relative to nearby free-face features.

Figure 4: Position of the site relative to nearby buildings and vegetation.

Figure 5: Street view of the flat land.

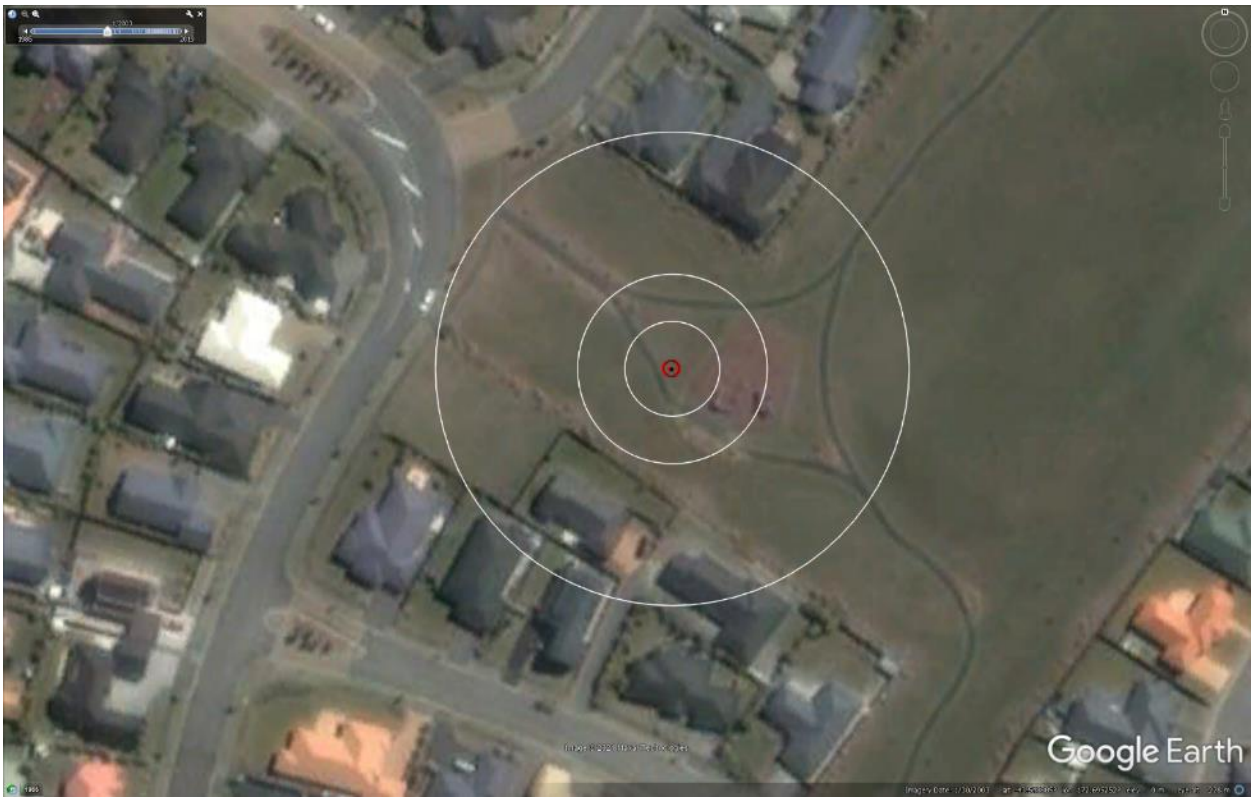

Figure 6: Satellite image of the site taken in Jan 2003.

Figure 7: Satellite image of the site taken in Dec 2004.

Figure 8: Satellite image of the site taken in Mar 2009.

Figure 9: Satellite image of the site taken in Oct 2009.

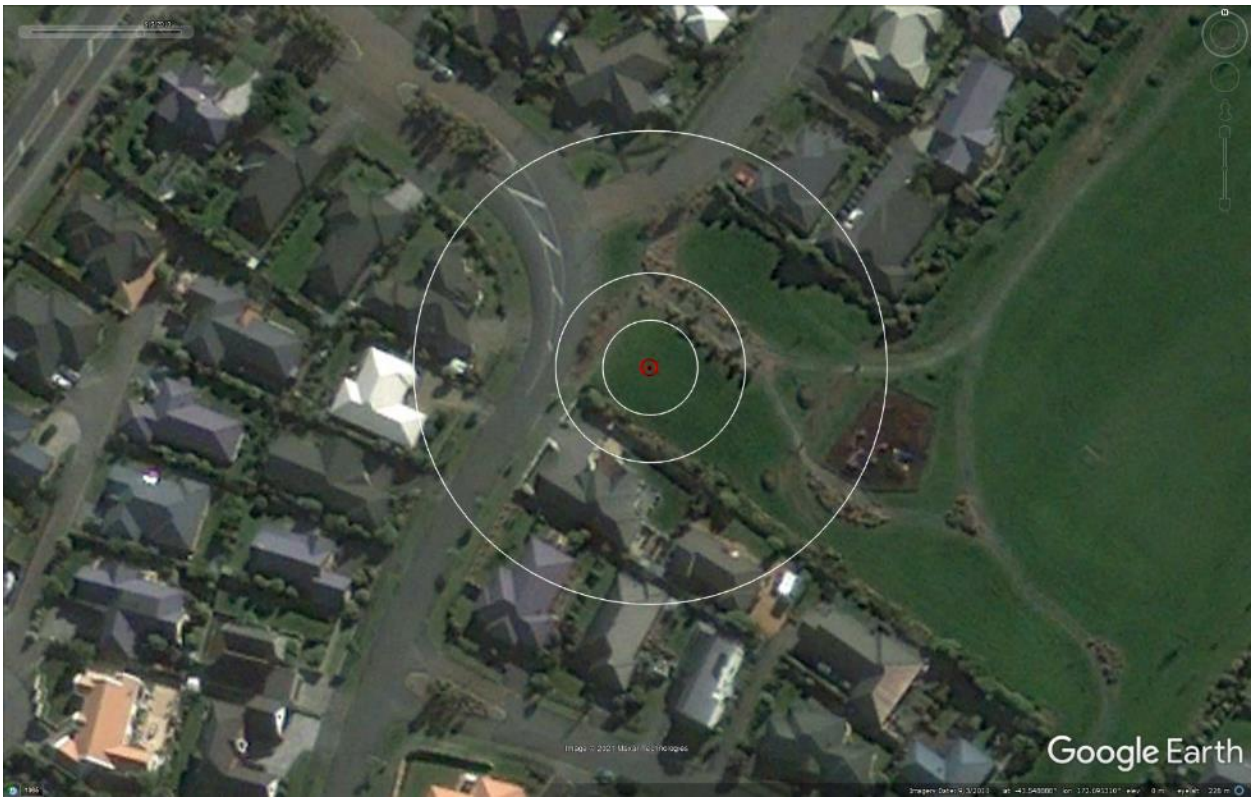

Figure 10: Satellite image of the site taken on Sep 3, 2010.

Figure 11: Satellite image of the site taken on Sep 5, 2010.

Figure 12: Satellite image of the site taken on Feb 15, 2011.

Figure 13: Satellite image of the site taken on Feb 23, 2011.

Figure 14: Satellite image of the site taken on Feb 26, 2011.

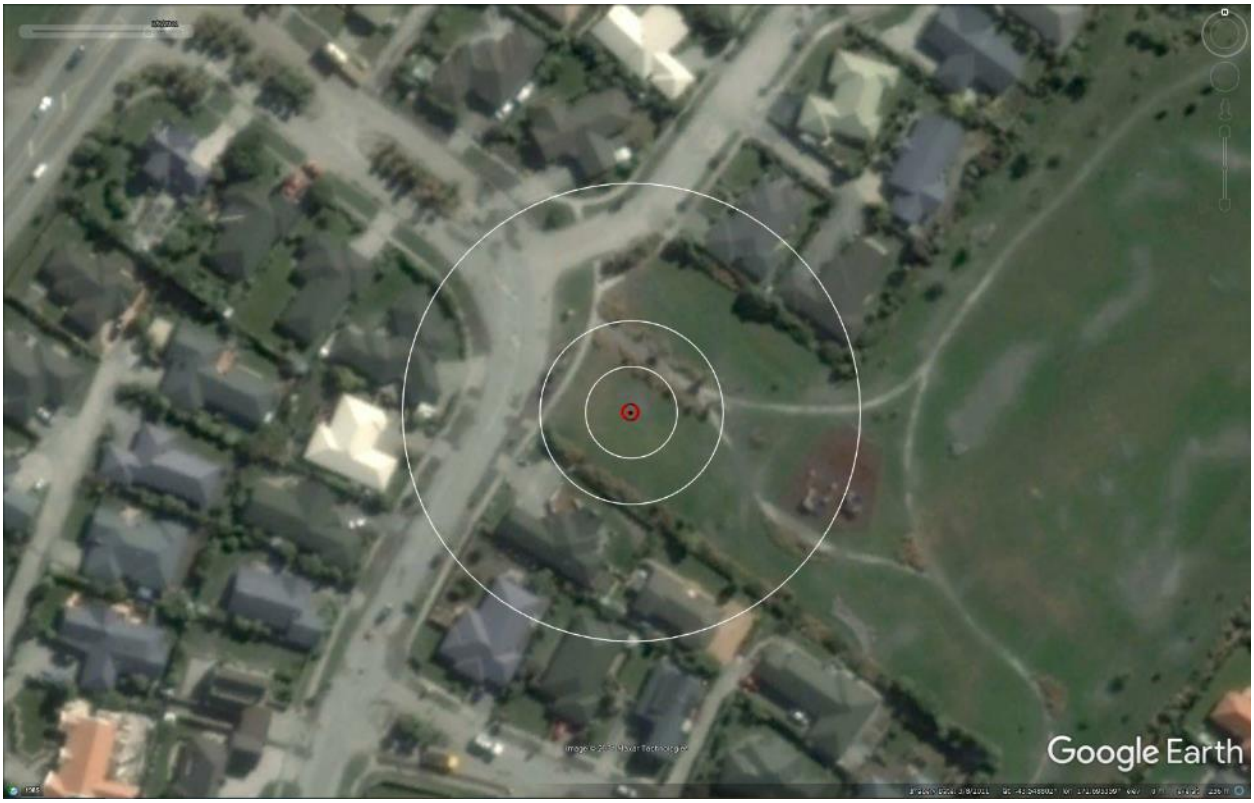

Figure 15: Satellite image of the site taken on Mar 8, 2011.

Figure 16: Satellite image of the site taken in Apr 2012.

Figure 17: Satellite image of the site taken in Mar 2013.

Figure 18: Satellite image of the site taken in Aug 2013.

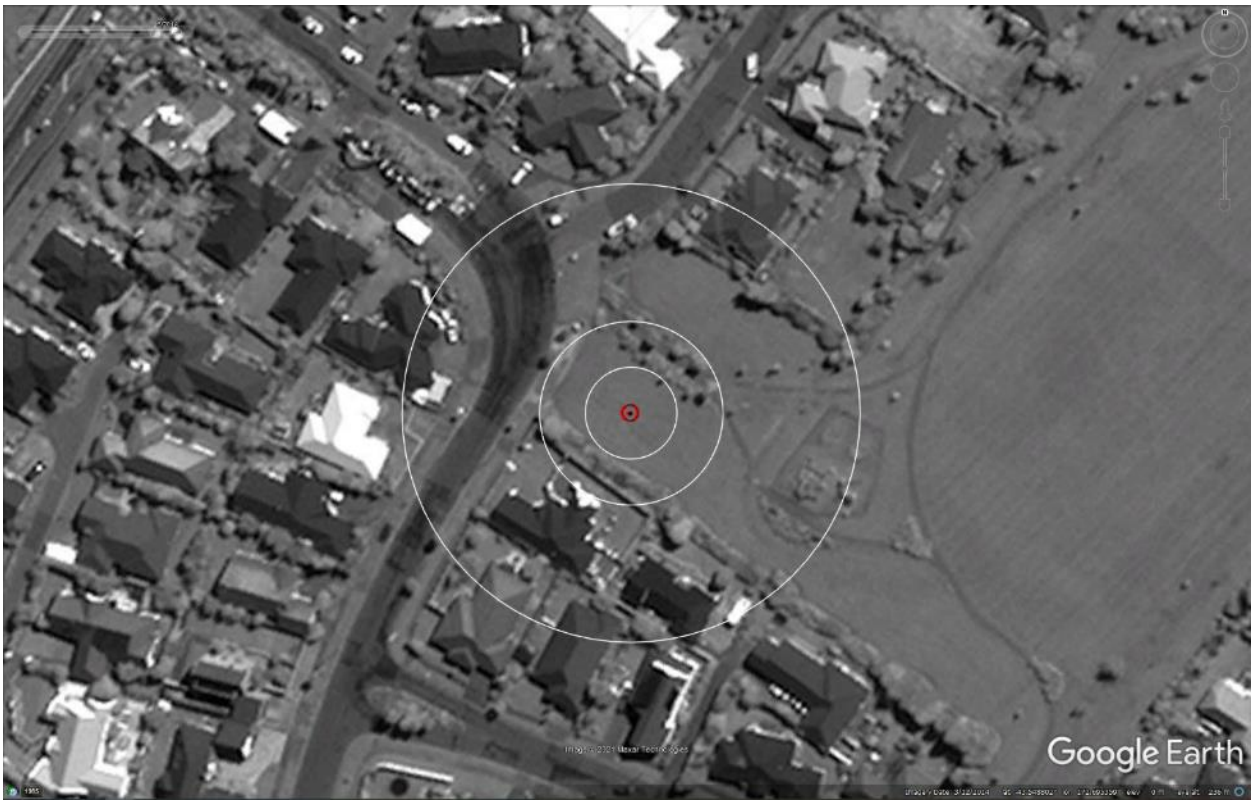

Figure 19: Satellite image of the site taken in Mar 2014.

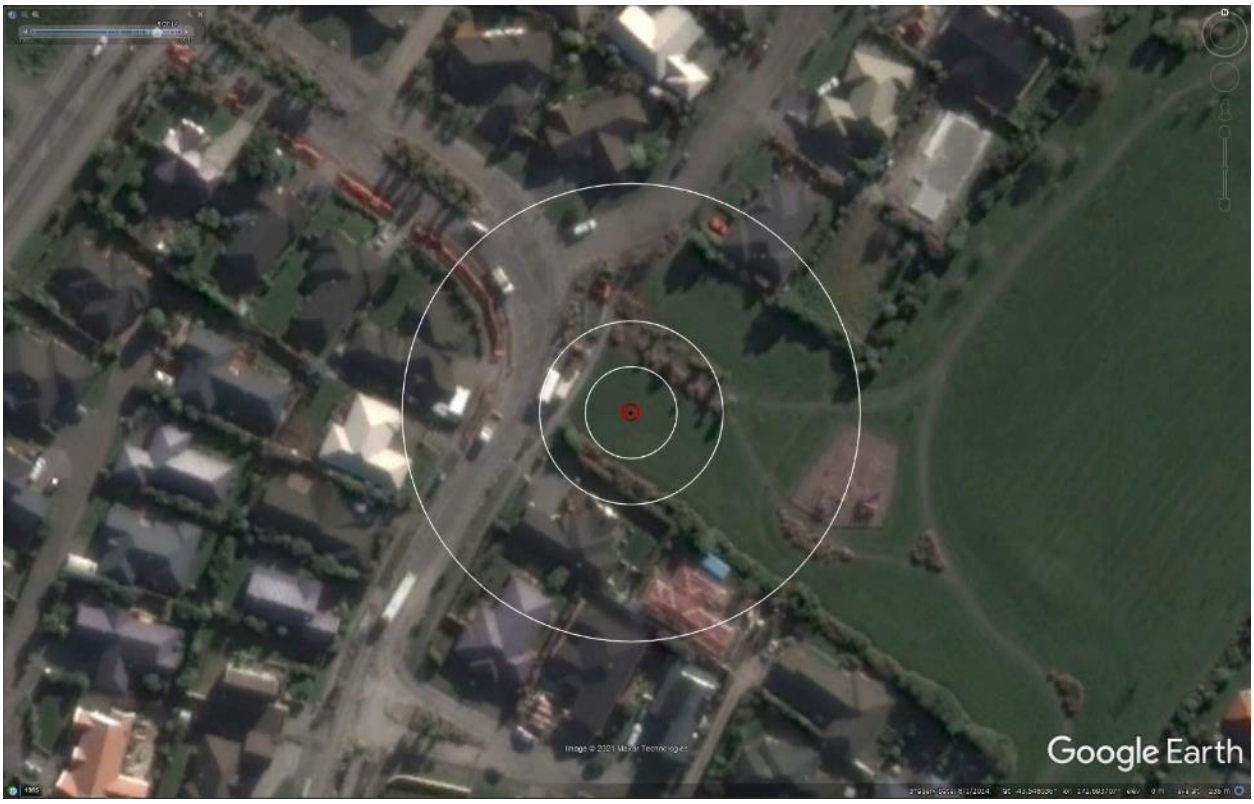

Figure 20: Satellite image of the site taken in Aug 2014.

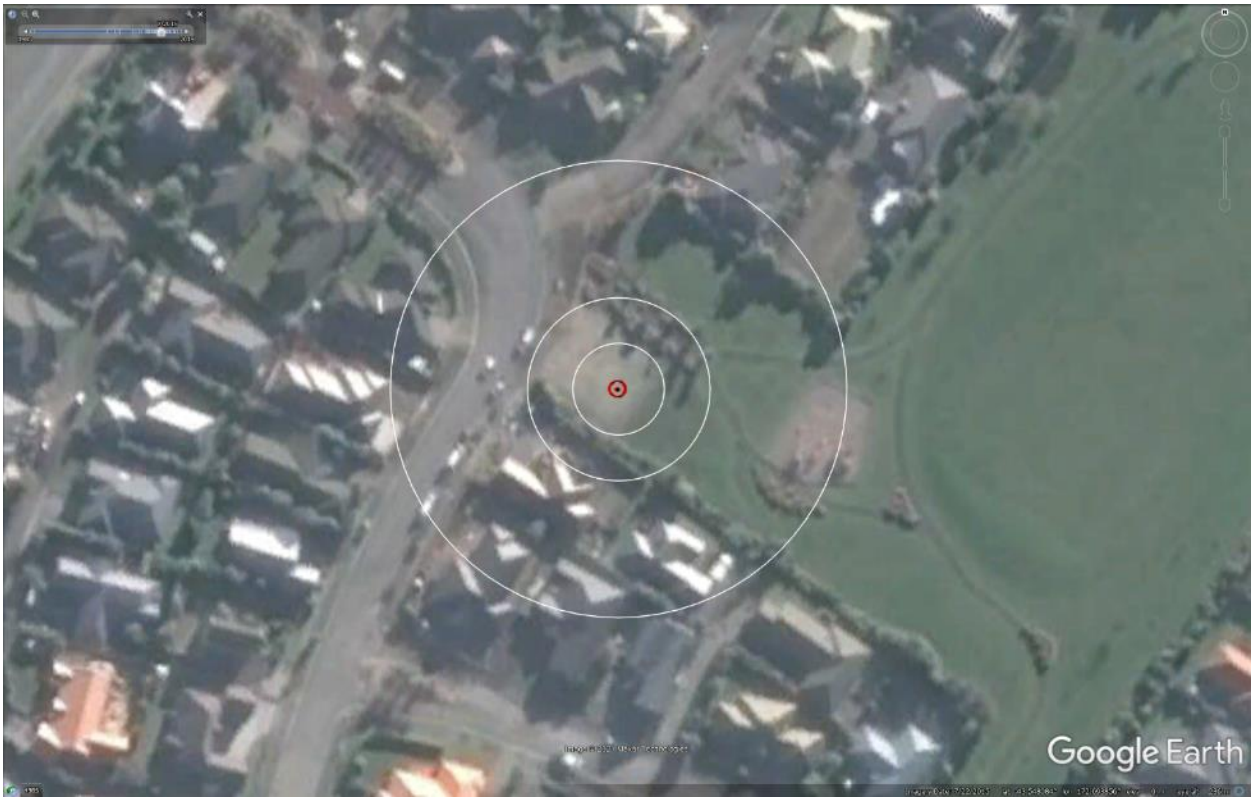

Figure 21: Satellite image of the site taken in Jul 2015.

Figure 22: Satellite image of the site taken in Nov 2015.

Figure 23: No aerial photograph of the site was acquired on Sep 4, 2010.

Figure 24: Aerial photograph of the site taken on Feb 24, 2011.

Figure 25: Aerial photograph of the site taken on June 14-15, 2011.

Figure 26: Aerial photograph of the site taken on June 16, 2011.

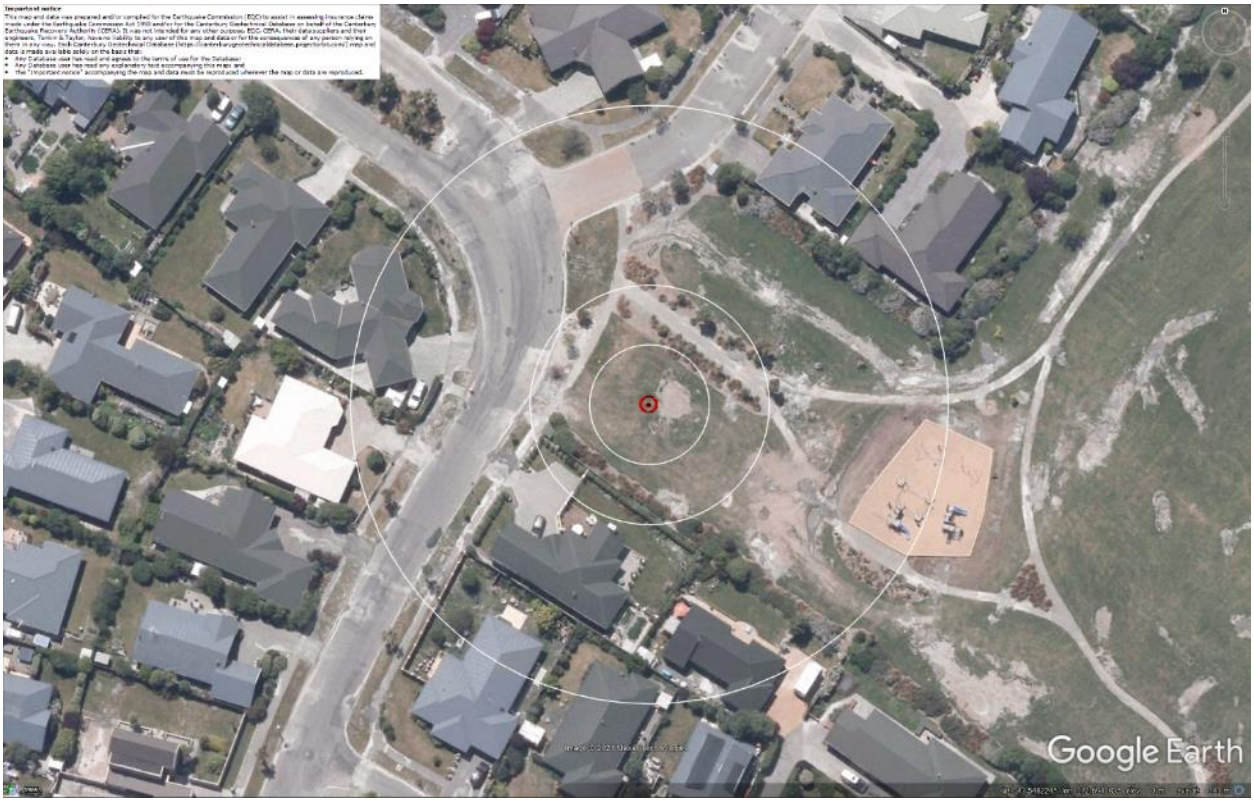

Figure 27: Aerial photograph of the site taken on Dec 24, 2011.

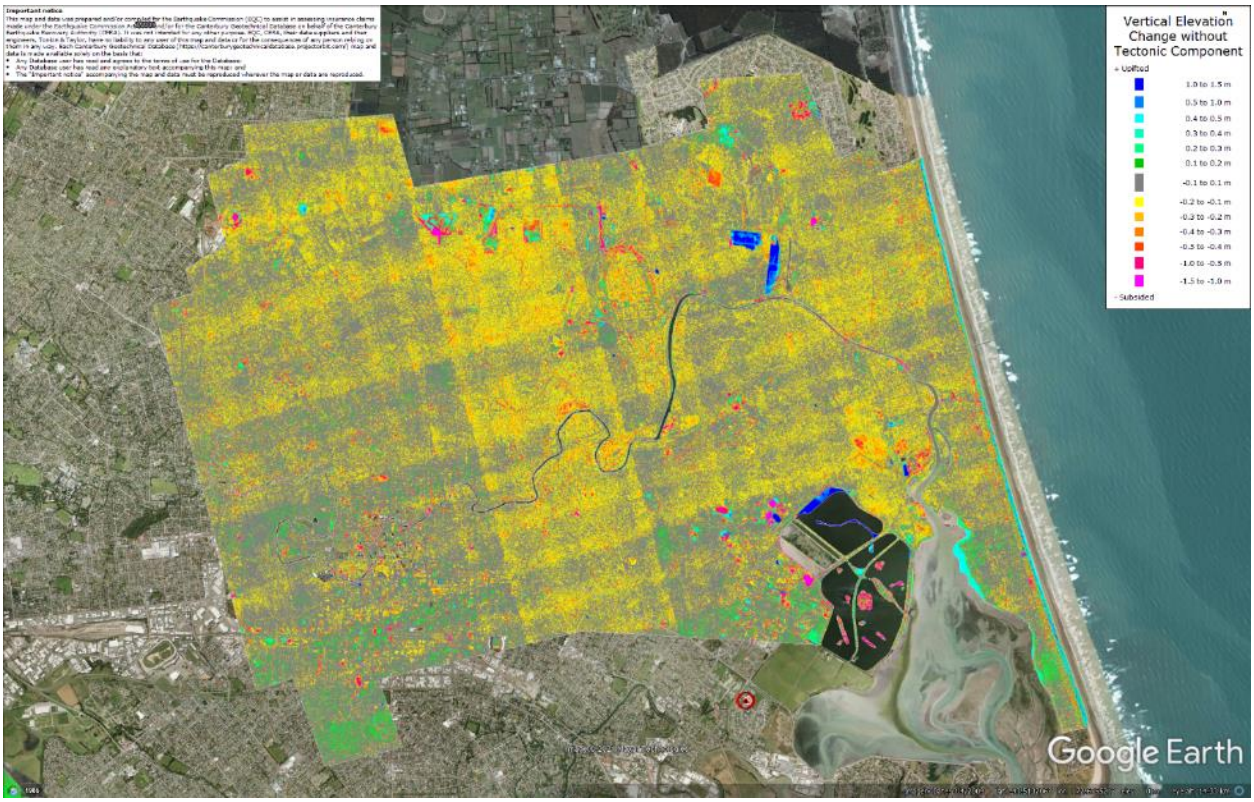

Figure 28: Vertical Ground Movements (Surface – Tectonic) for Sep 2010 Earthquake are not available due to the absence of Sep 2010 LiDAR survey for the site.

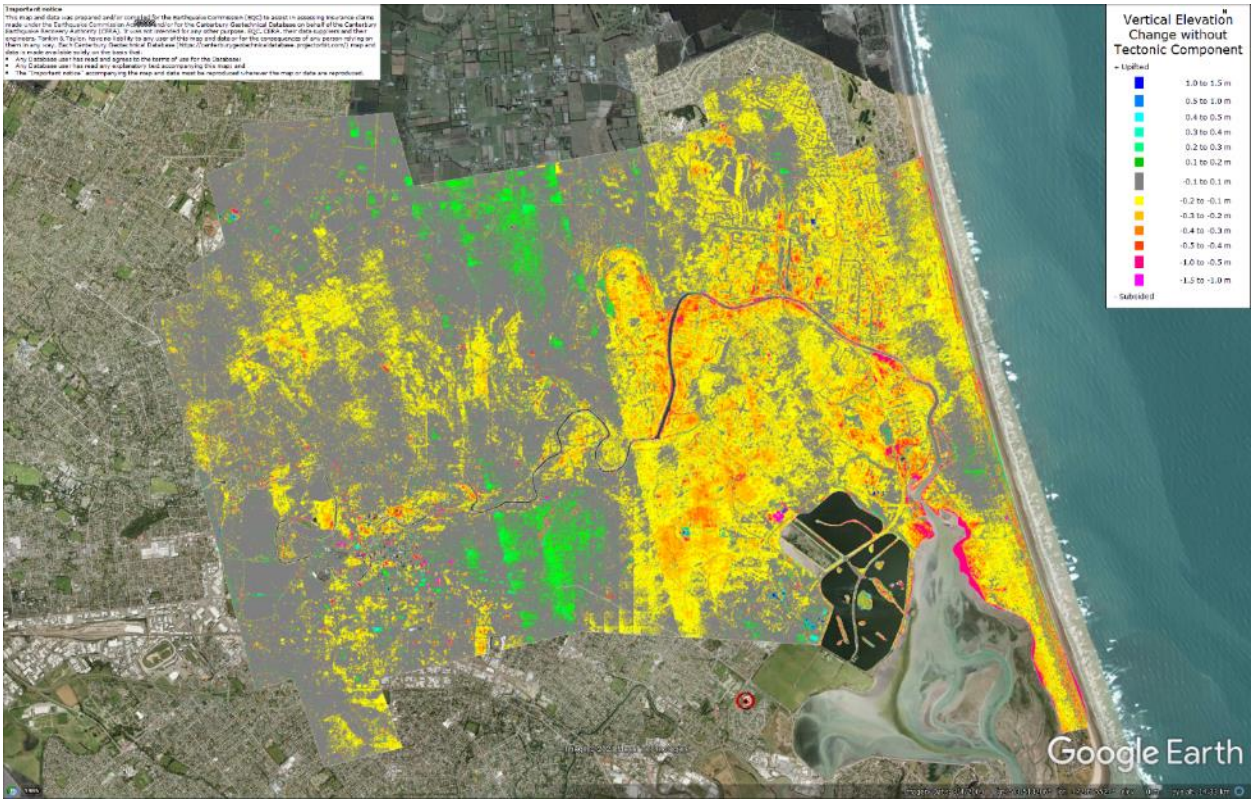

Figure 29: Vertical Ground Movements (Surface – Tectonic) for Feb 2011 Earthquake are not available due to the absence of Sep 2010 LiDAR survey for the site.

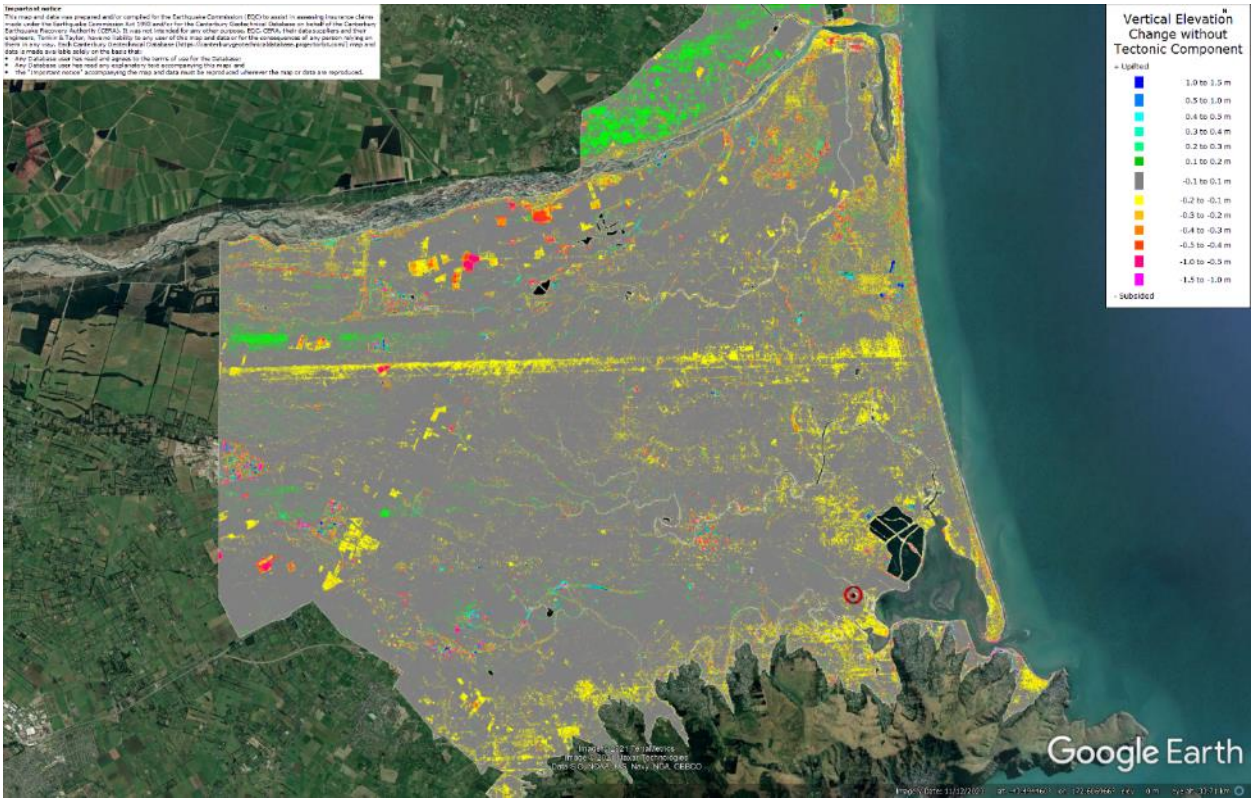

Figure 30: Vertical Ground Movements (Surface – Tectonic) for June 2011 Earthquake – the site is not in the apparent zone of overestimated or underestimated ground surface subsidence.

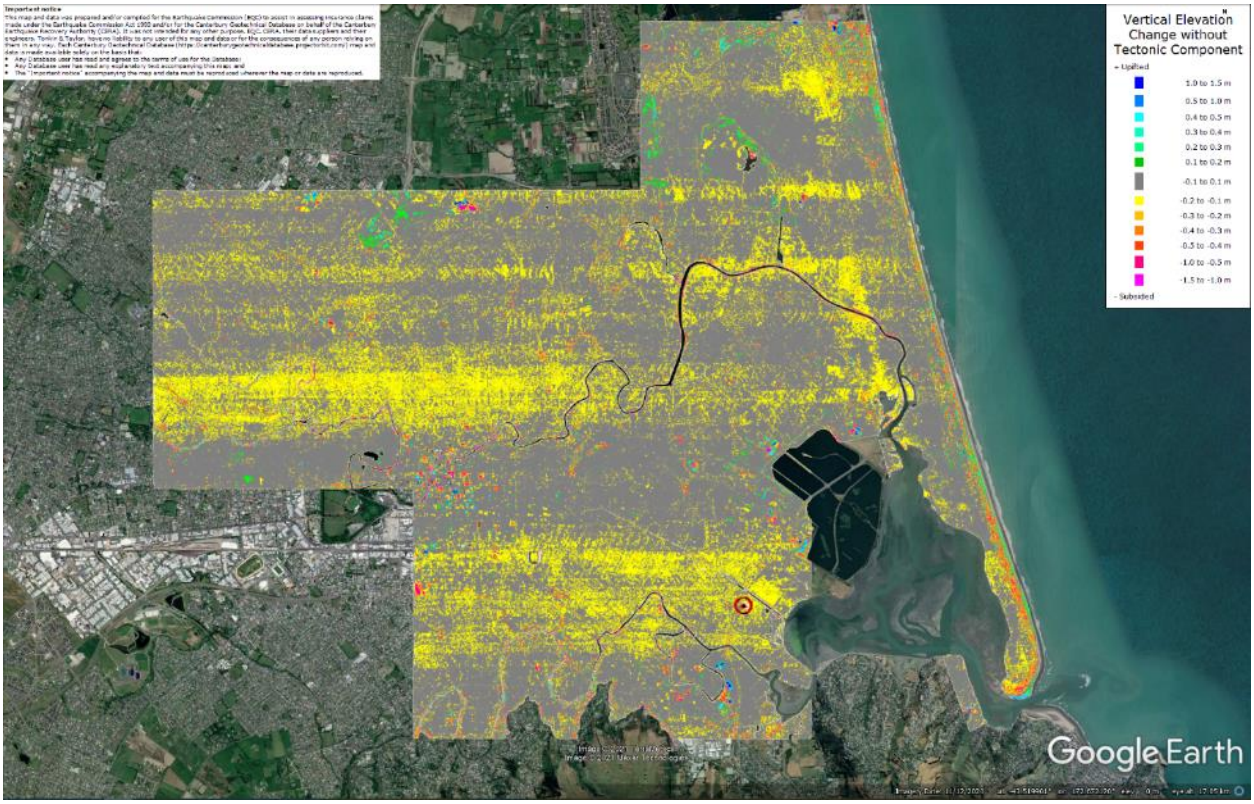

Figure 31: Vertical Ground Movements (Surface – Tectonic) for Dec 2011 Earthquake – the site is in the apparent zone of overestimated ground surface subsidence (i.e., July 2003 flight path error).

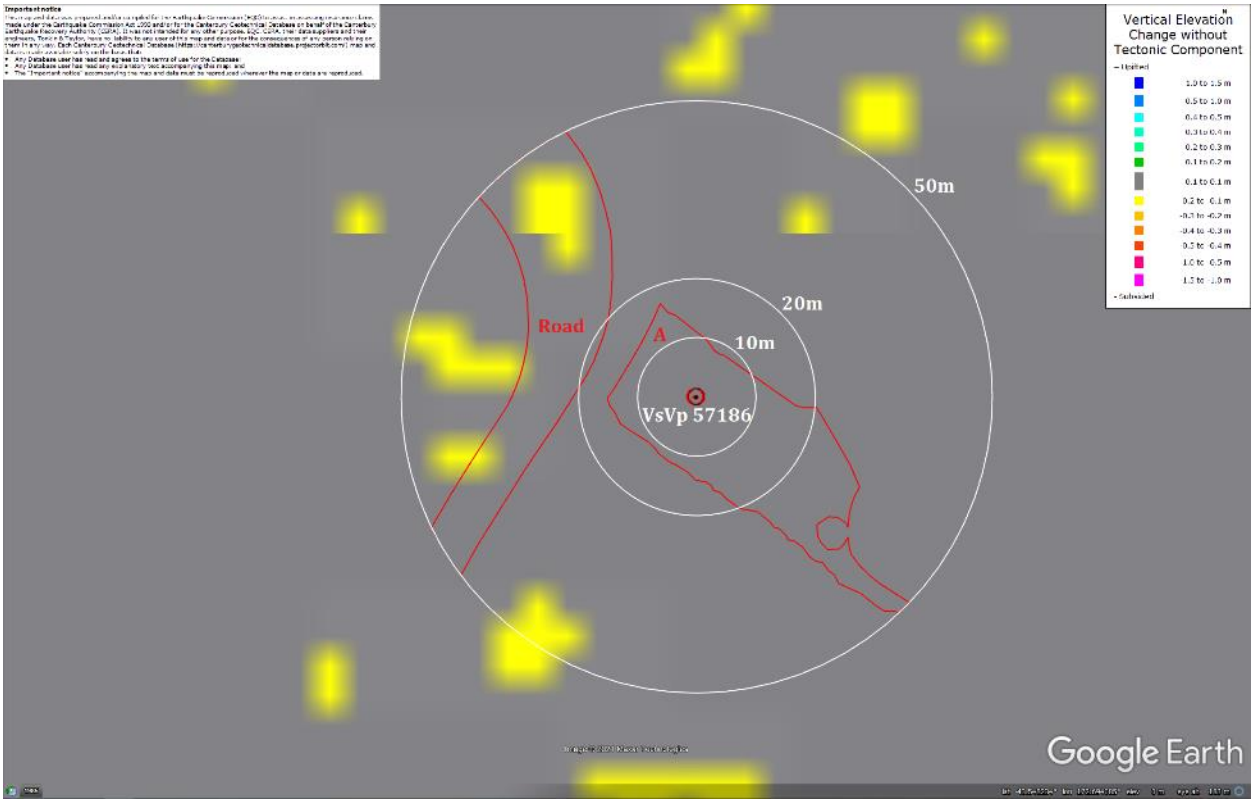

Figure 32: Ground surface subsidence without tectonic component for June 2011 Earthquake according to the LiDAR DEM.

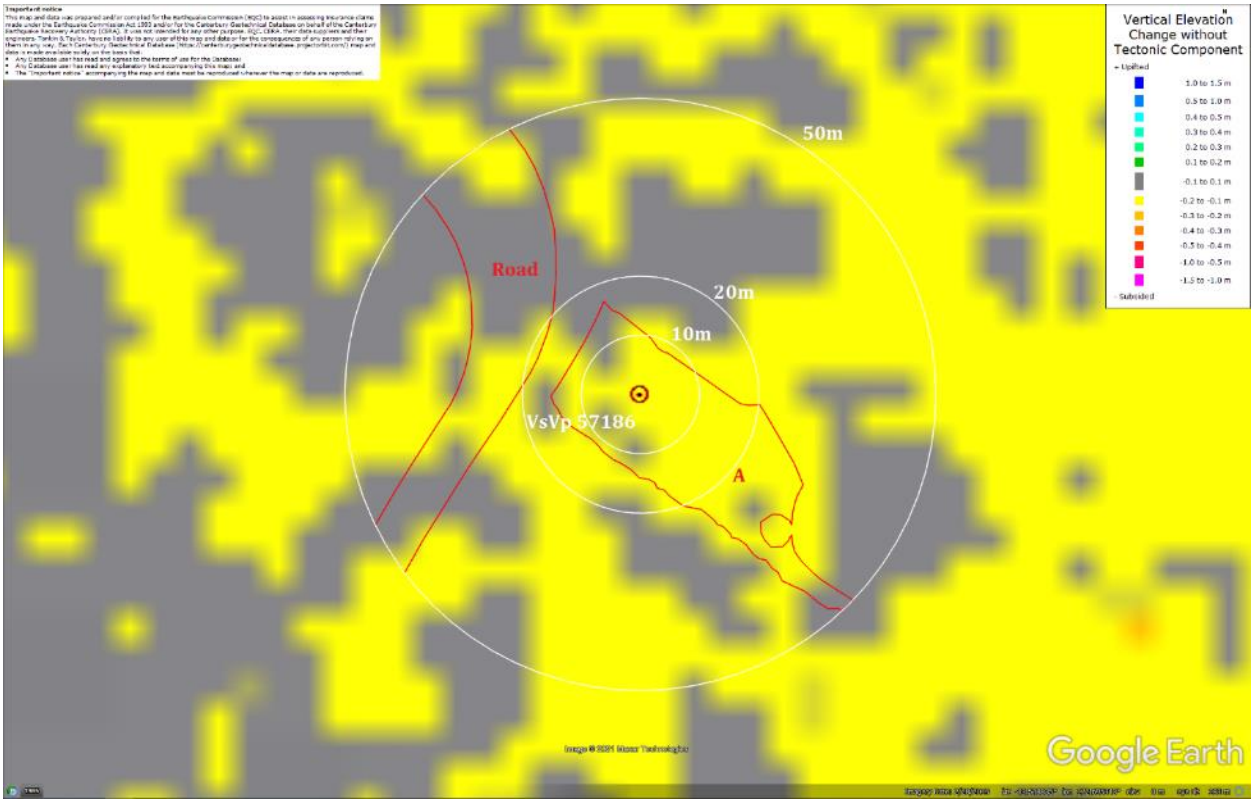

Figure 33: Ground surface subsidence without tectonic component for Dec 2011 Earthquake according to the LiDAR DEM.

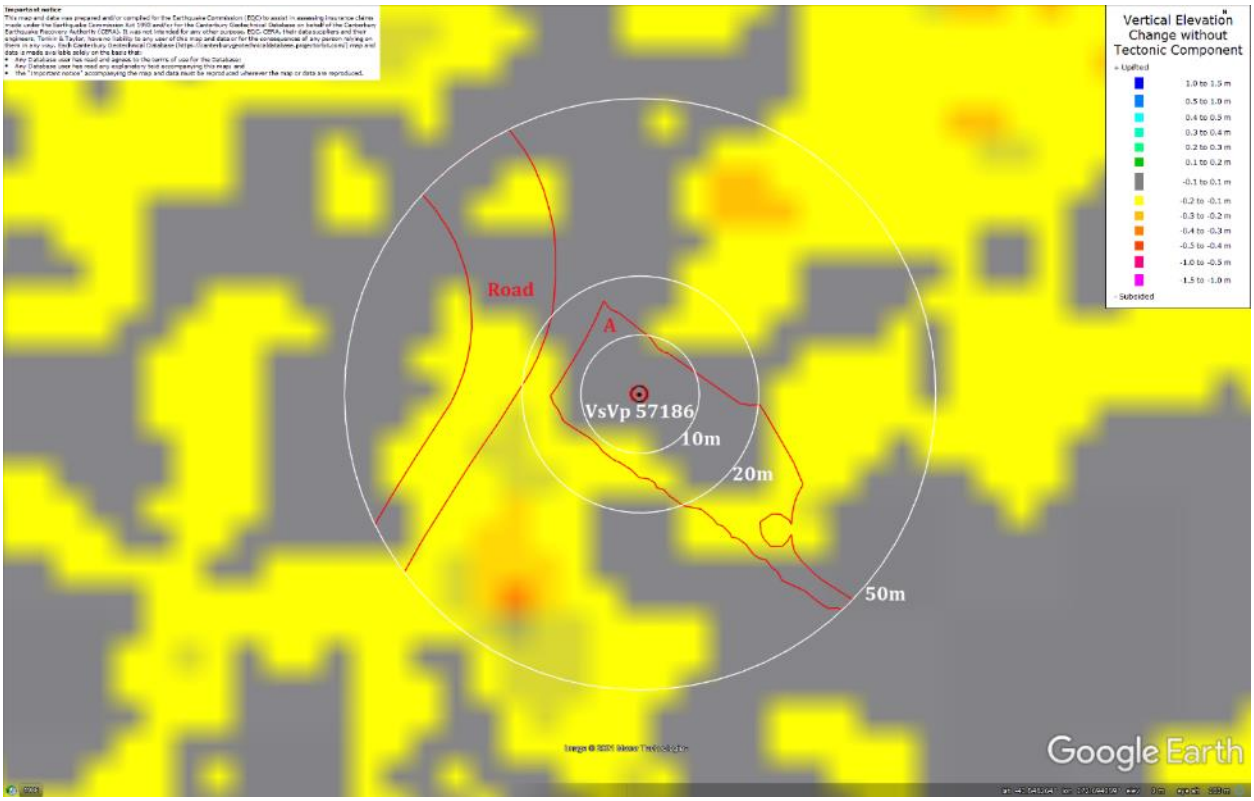

Figure 34: Ground surface subsidence without tectonic component for Canterbury Earthquake Sequence according to the LiDAR DEM.

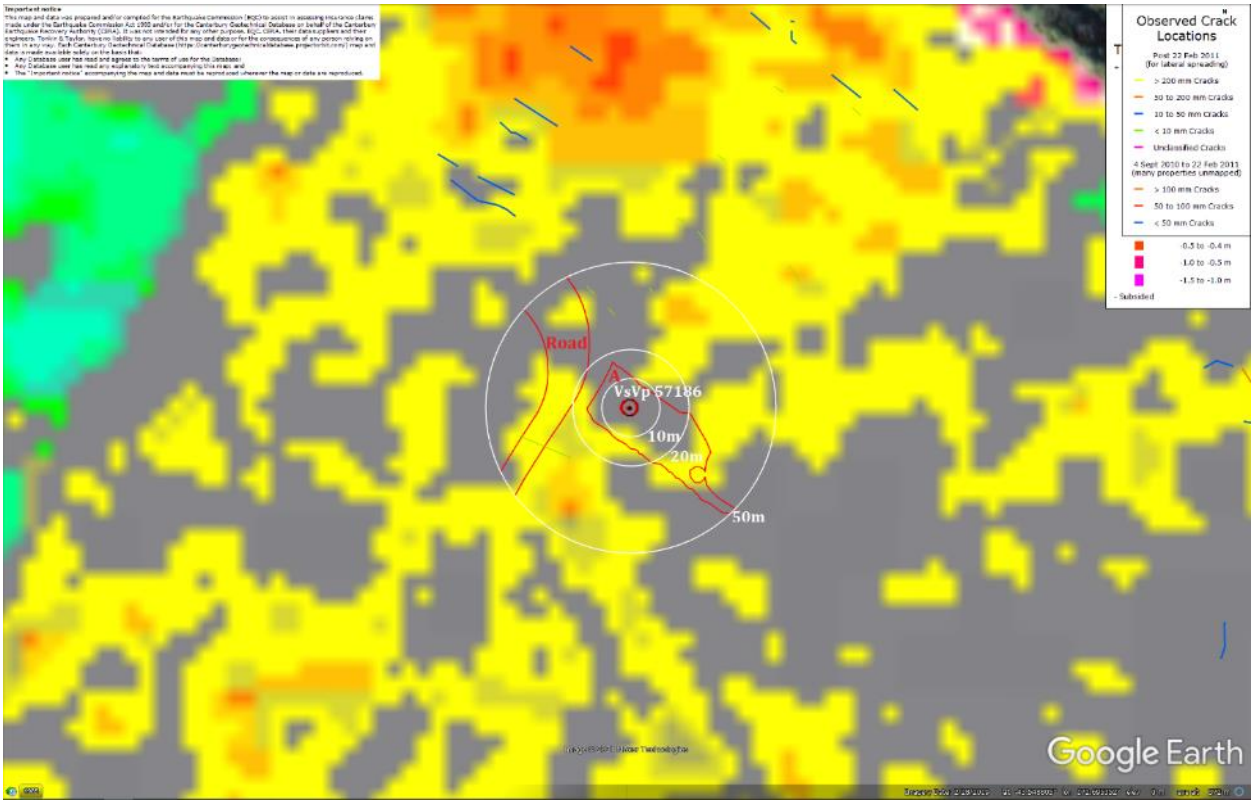

Figure 35: No lateral spreading for Canterbury Earthquake Sequence.

Figure 36: Vertical tectonic movements for Sep 2010 Earthquake.

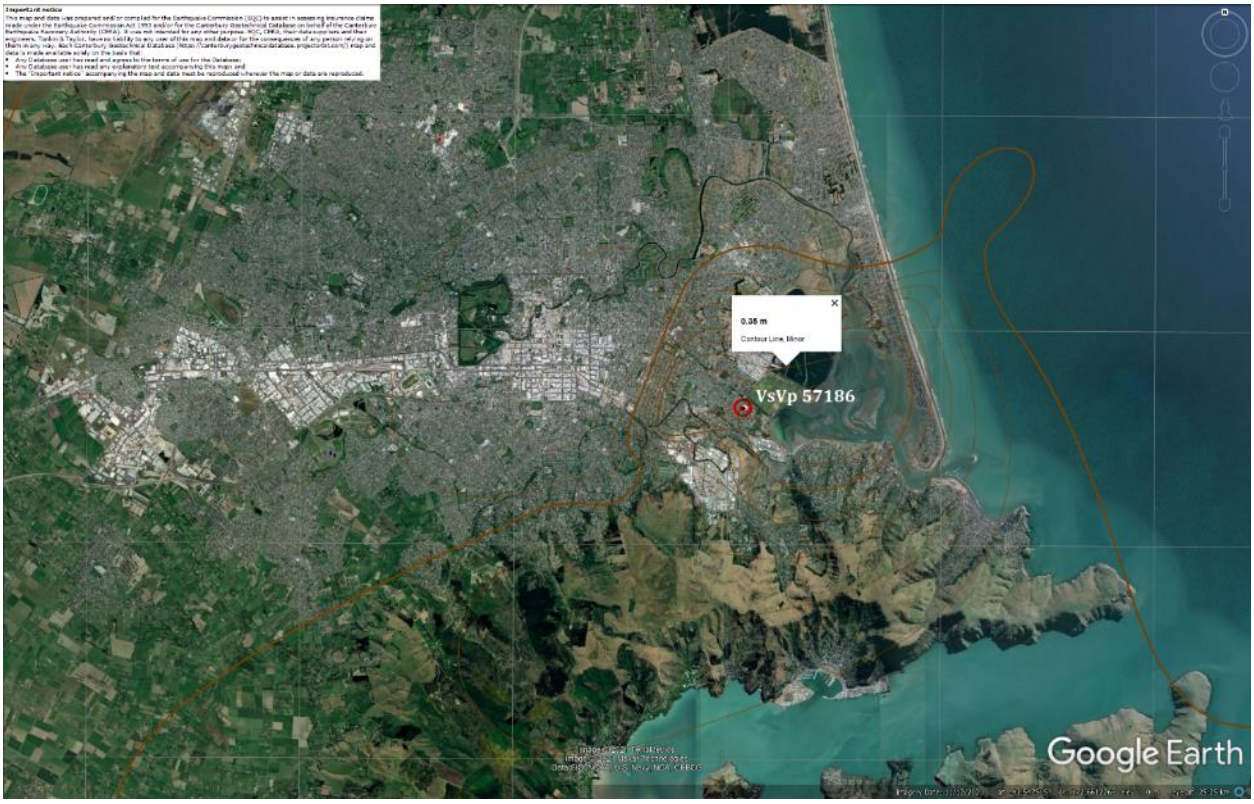

Figure 37: Vertical tectonic movements for Feb 2011 Earthquake.

Figure 38: Vertical tectonic movements for June 2011 Earthquake.

Figure 39: Vertical tectonic movements for Dec 2011 Earthquake.

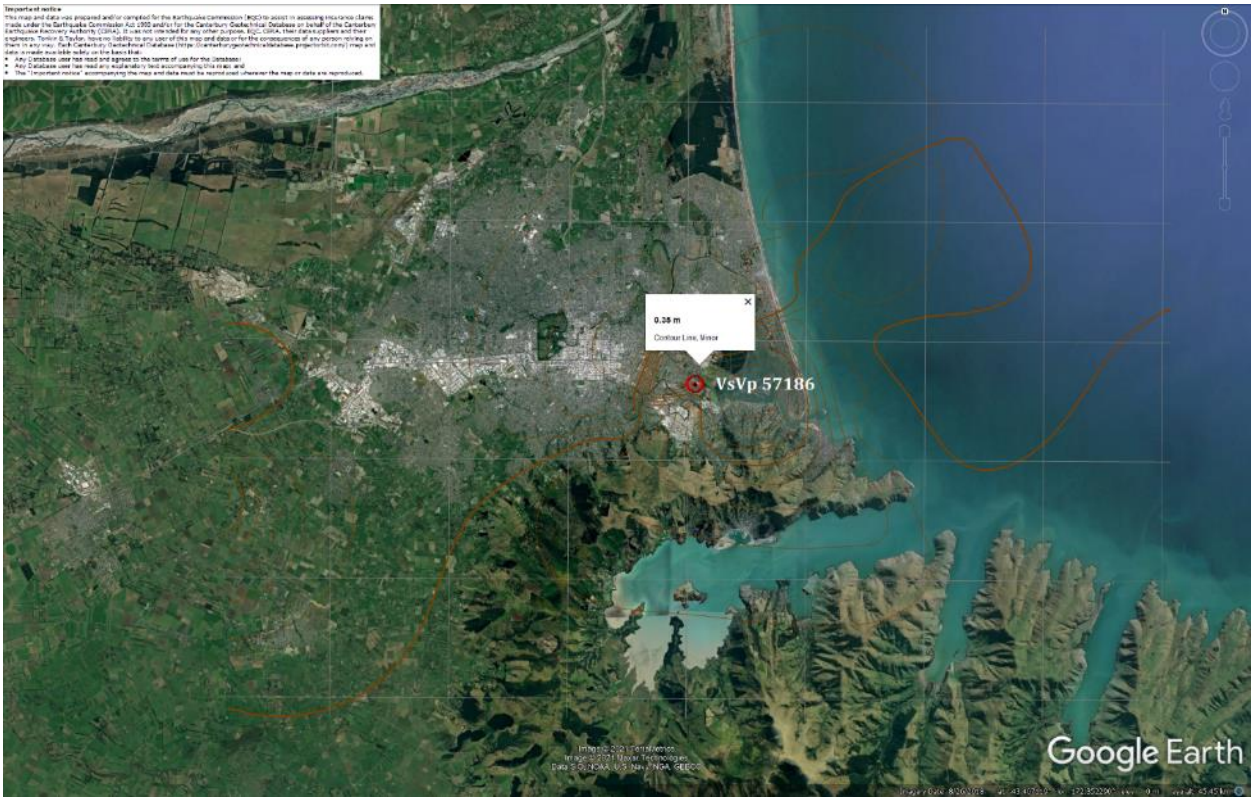

Figure 40: Vertical tectonic movements for Canterbury Earthquake Sequence.

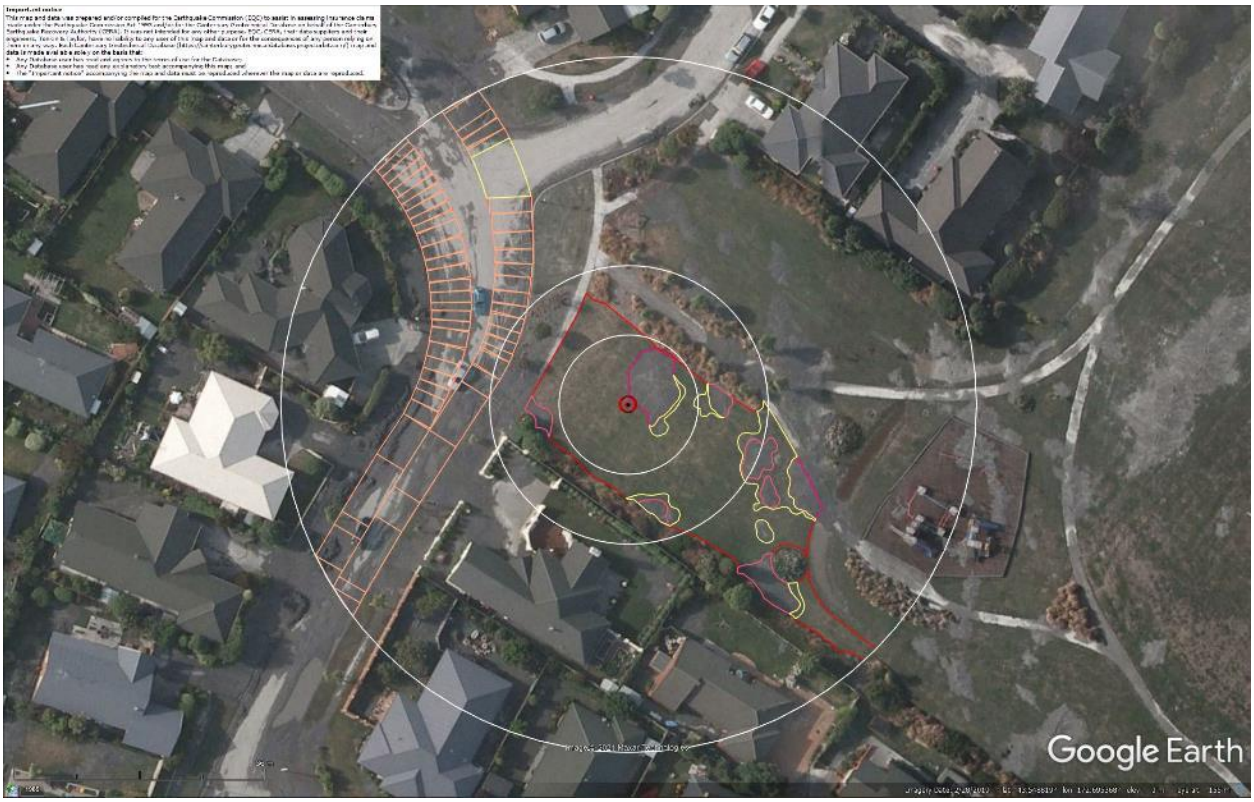

Figure 41: Aerial photograph showing the ejecta outline at the site for Feb-11 EQ.

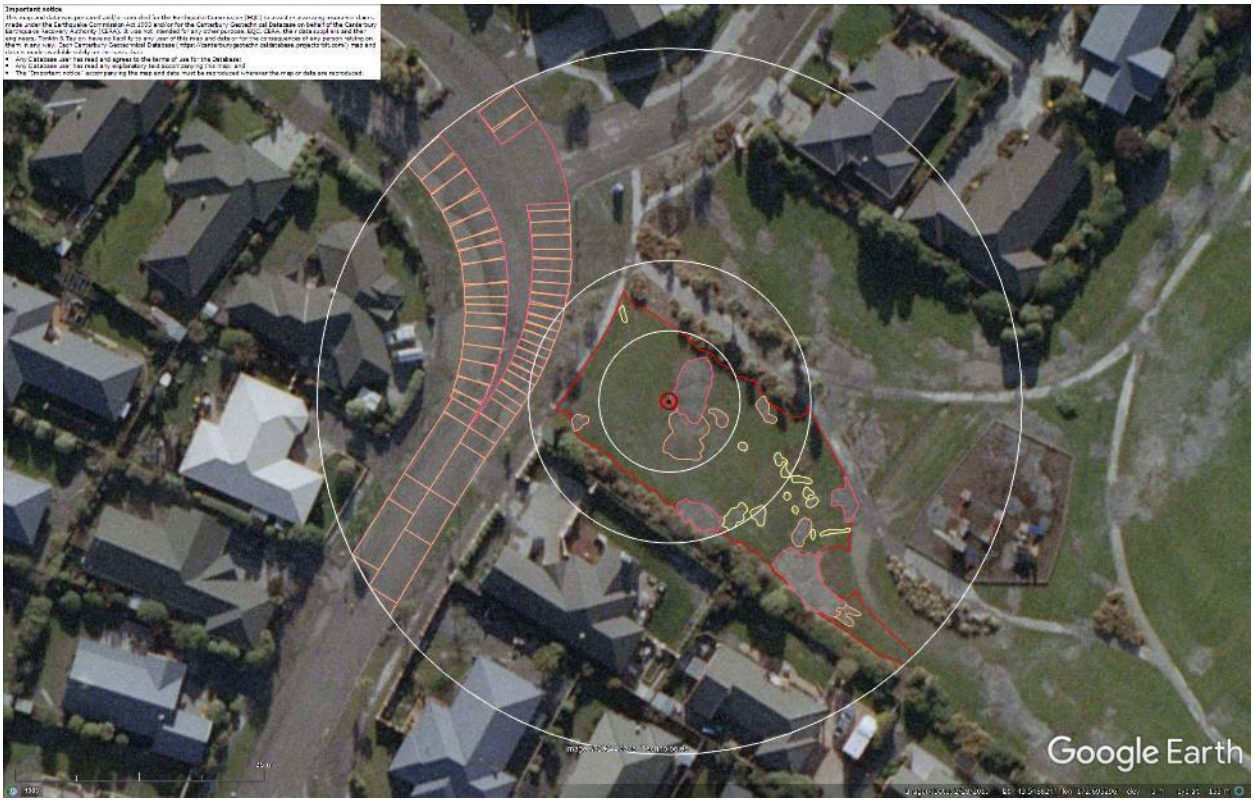

Figure 42: Aerial photograph acquired on 16 Jun 2011 showing the ejecta outline at the site for Jun-11 EQ.

Figure 43: Aerial photograph showing the ejecta outline at the site for Dec-11 EQ.

Contents of this figure cannot be shared as doing so is restricted by a Non-Disclosure Agreement.

Figure 44: LDAT inspection notes for the property in the N portion of the 50-m buffer (inspection date: Nov 2011).

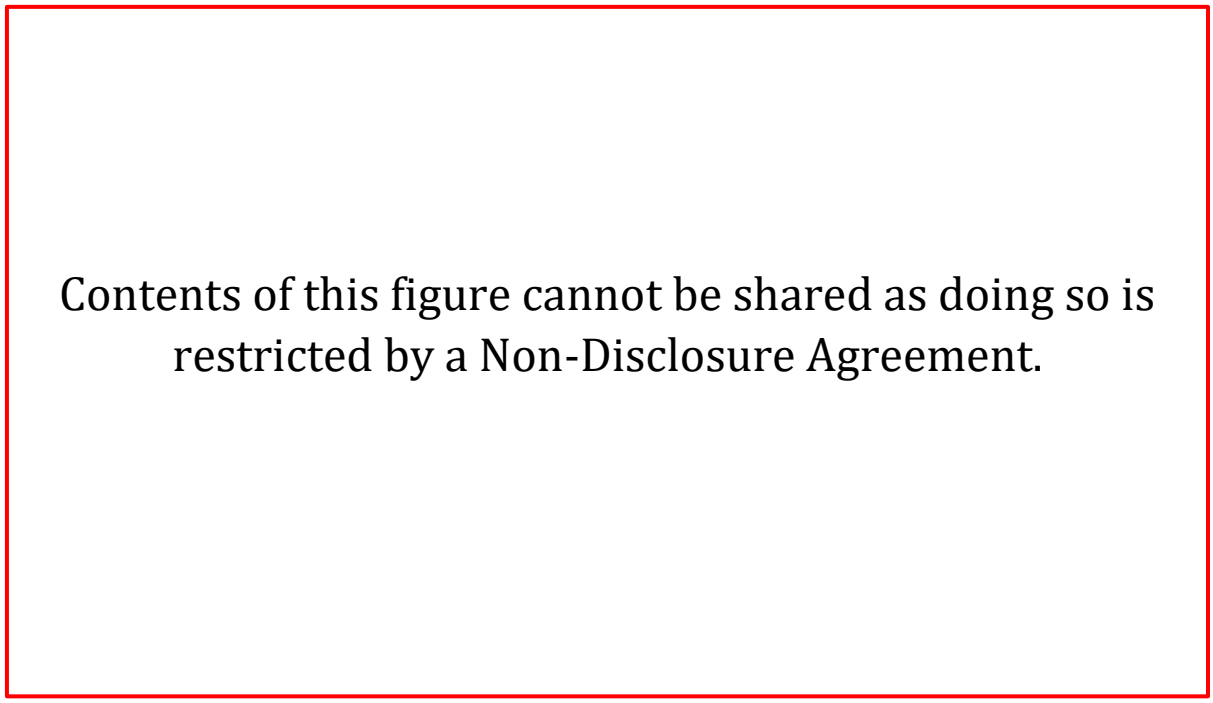

Figure 45: LDAT inspection notes for the property in the NE quadrant of the 50-m buffer (inspection date: Nov 2011). The height of the ejecta remnants ranged from 50 mm to 100 mm.

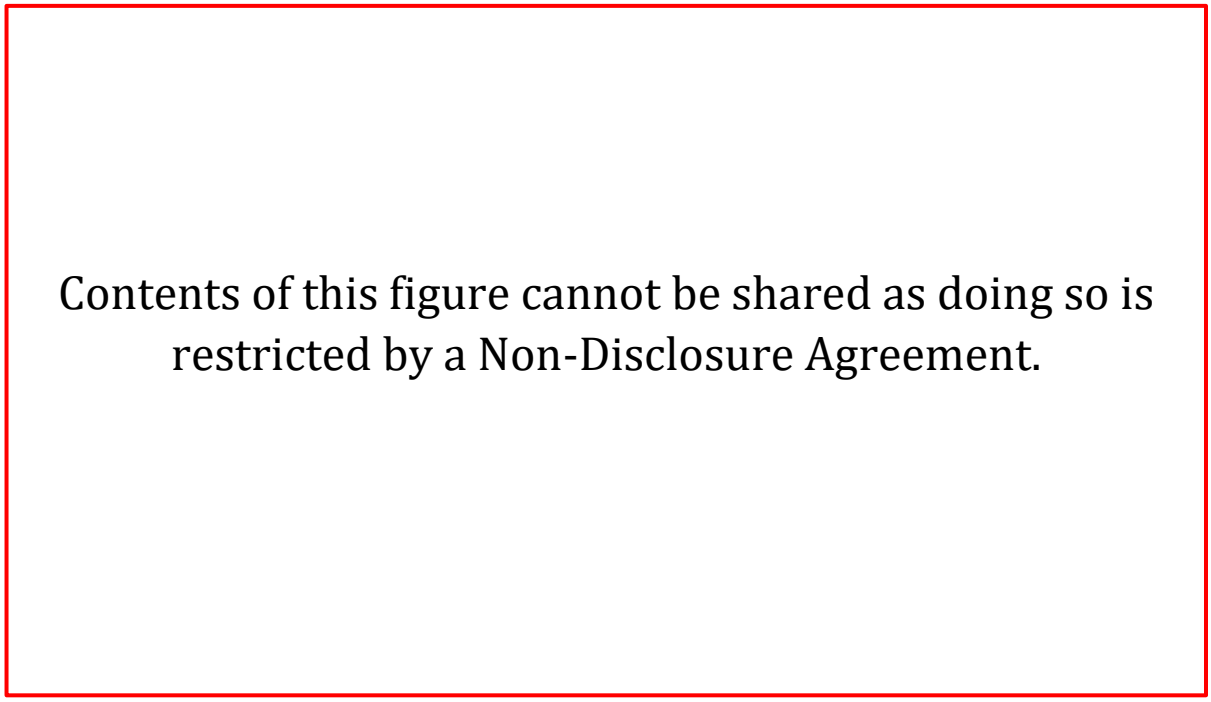

Figure 46: LDAT inspection notes for the property in the NE portion of the 50-m buffer (inspection date: Nov 2011). The height of the ejecta remnants ranged from 100 mm to 300 mm.

Figure 47: Ground photographs of ejecta on the properties in the NE quadrant of the 50-m buffer (photograph date: Nov 2011).

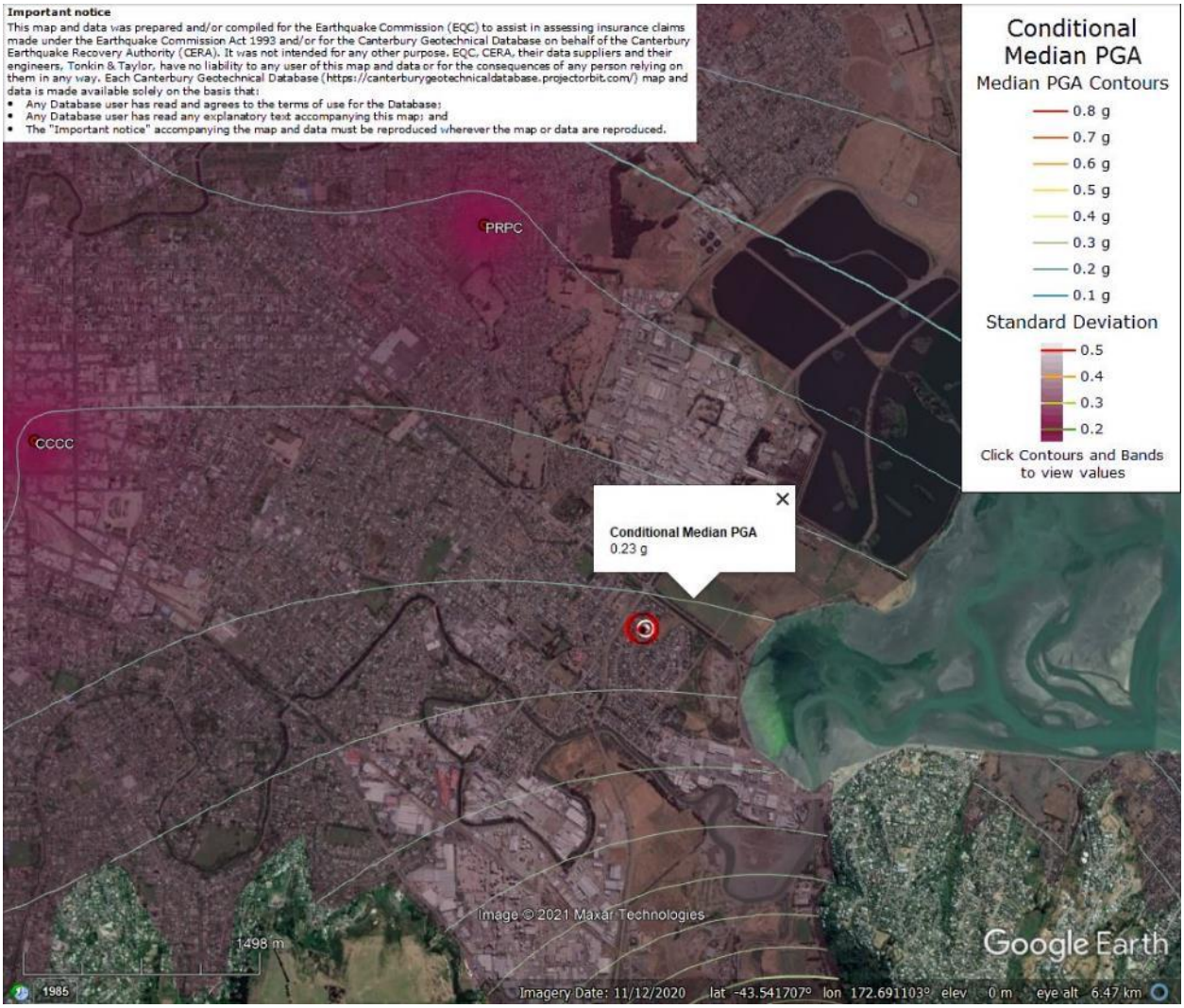

Figure 48: PGA for Sep-10 EQ (st. dev. = 0.350-0.375 ln units).

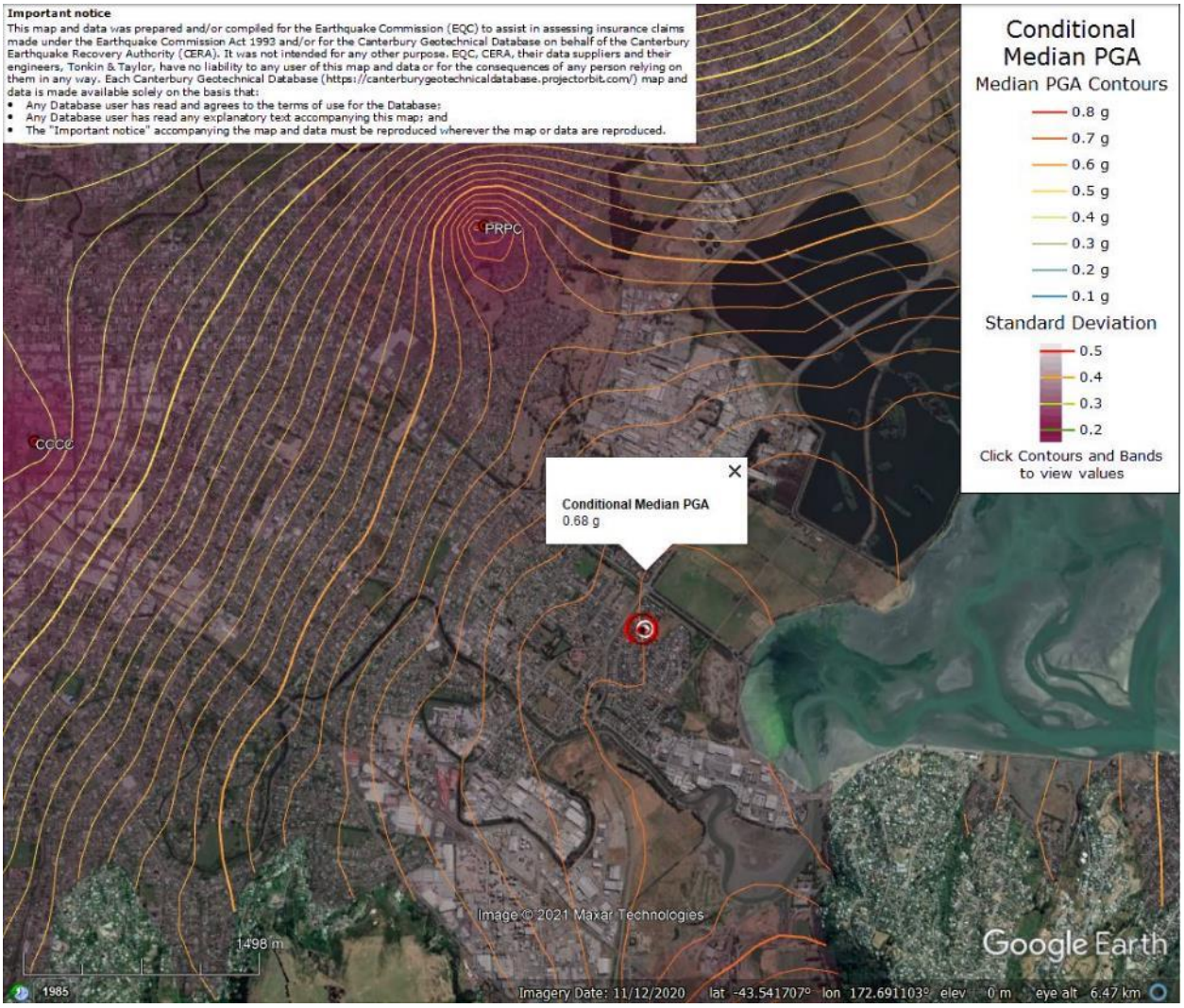

Figure 49: PGA for Feb-11 EQ (st. dev. = 0.375-0.400 ln units).

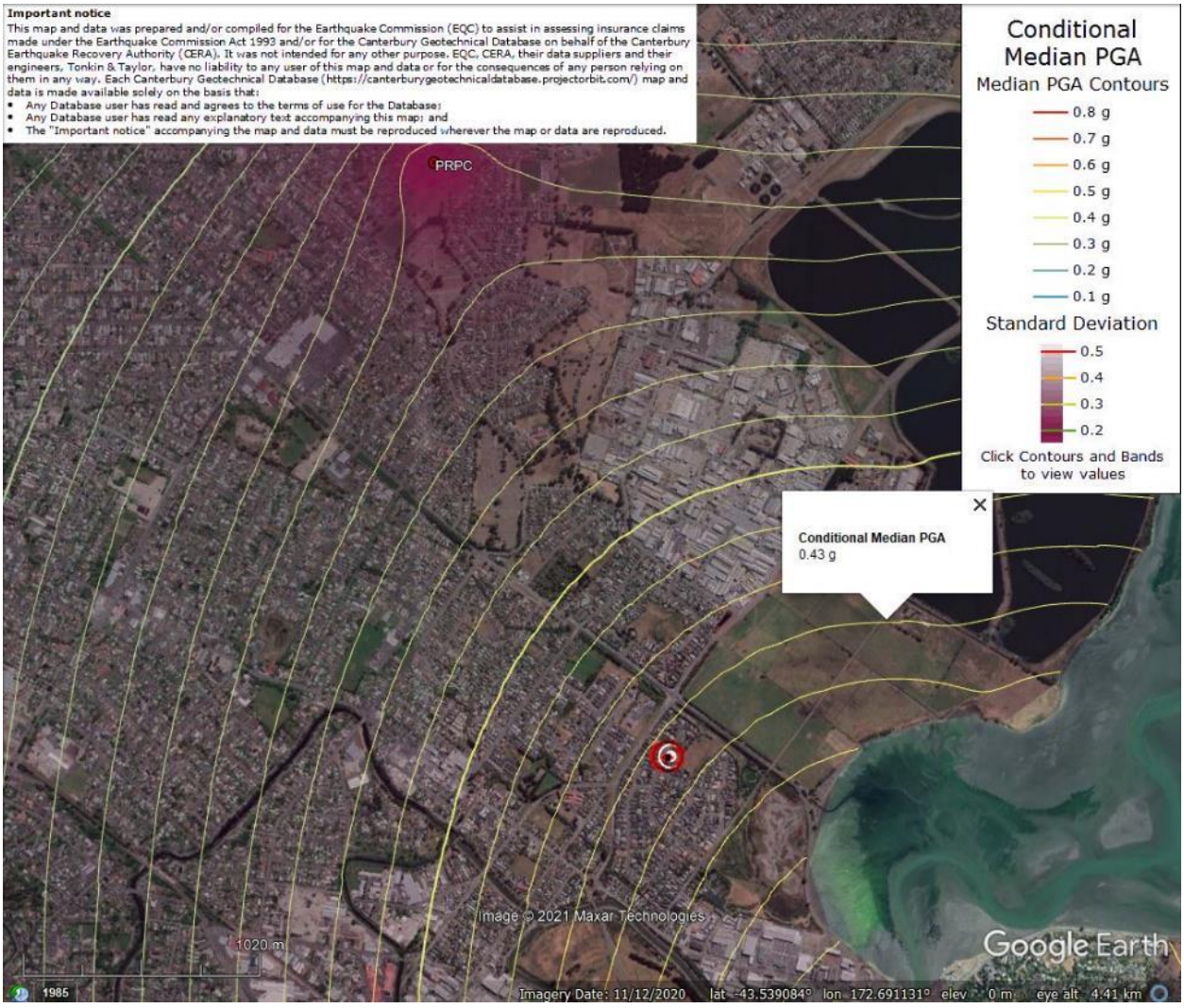

Figure 50: PGA for Jun-11 EQ (st. dev. = 0.400-0.425 ln units).

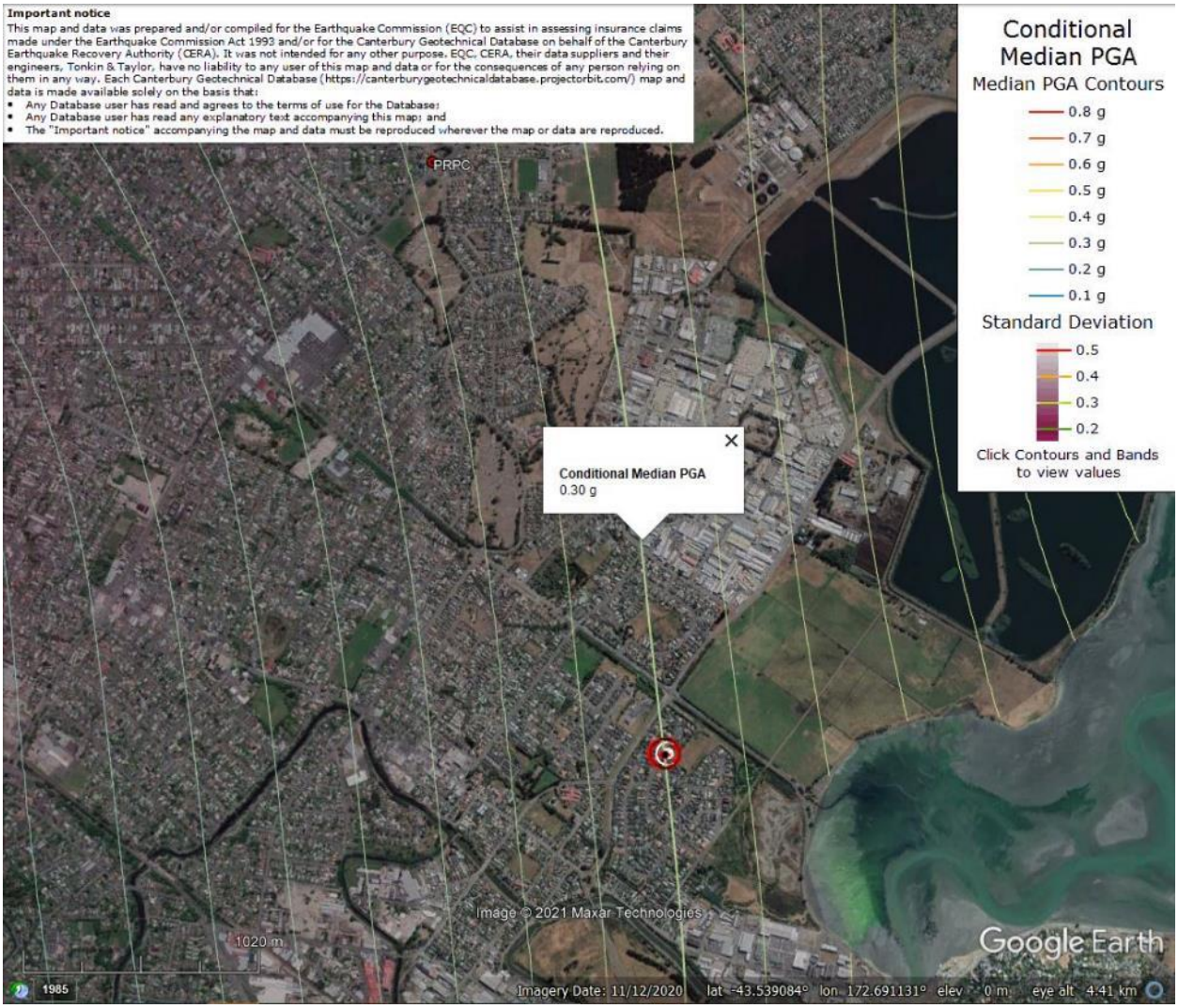

Figure 51: PGA for Dec-11 EQ (st. dev. = 0.425-0.450 ln units).

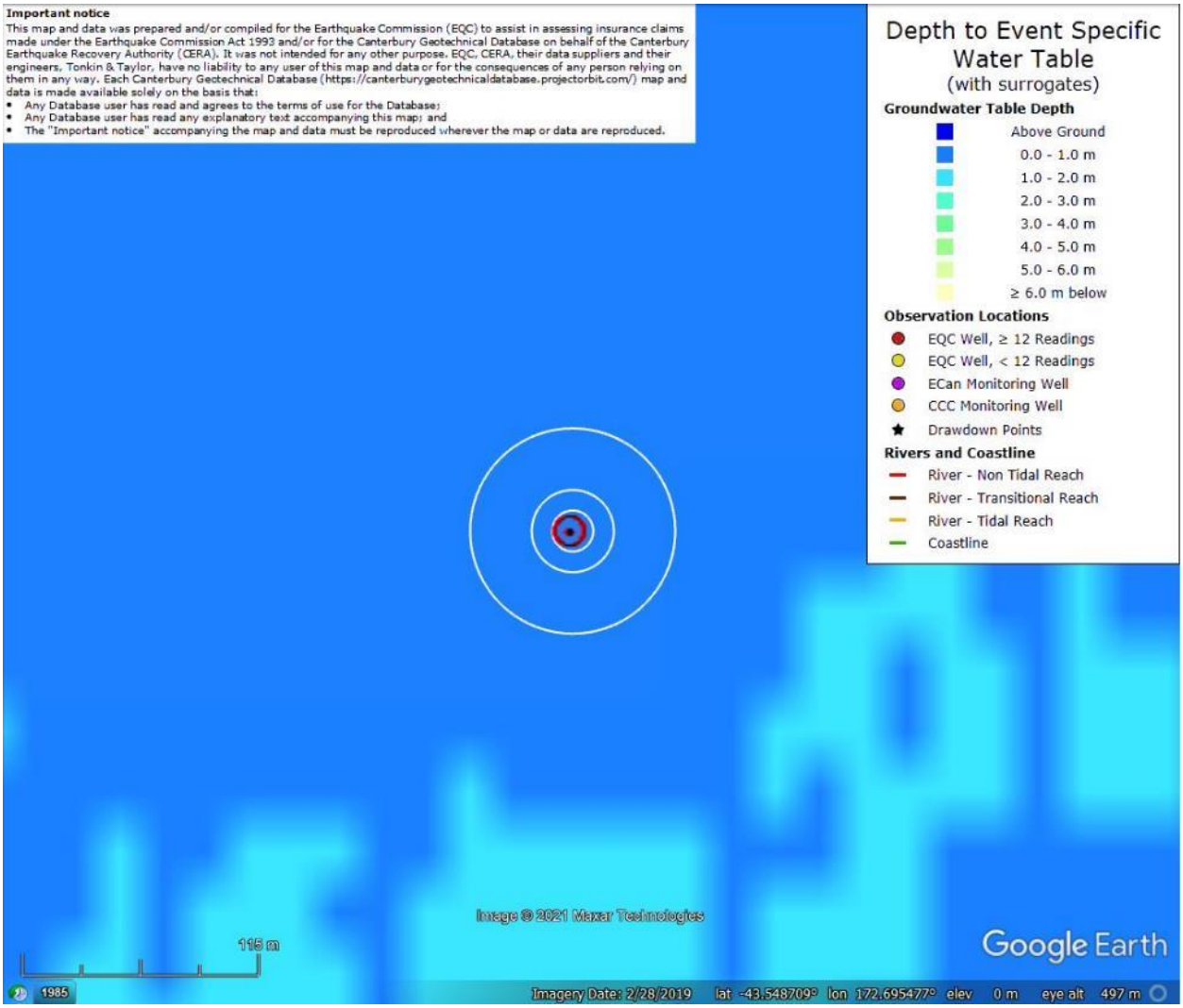

Figure 52: Depth to groundwater table for Sep-10 EQ.

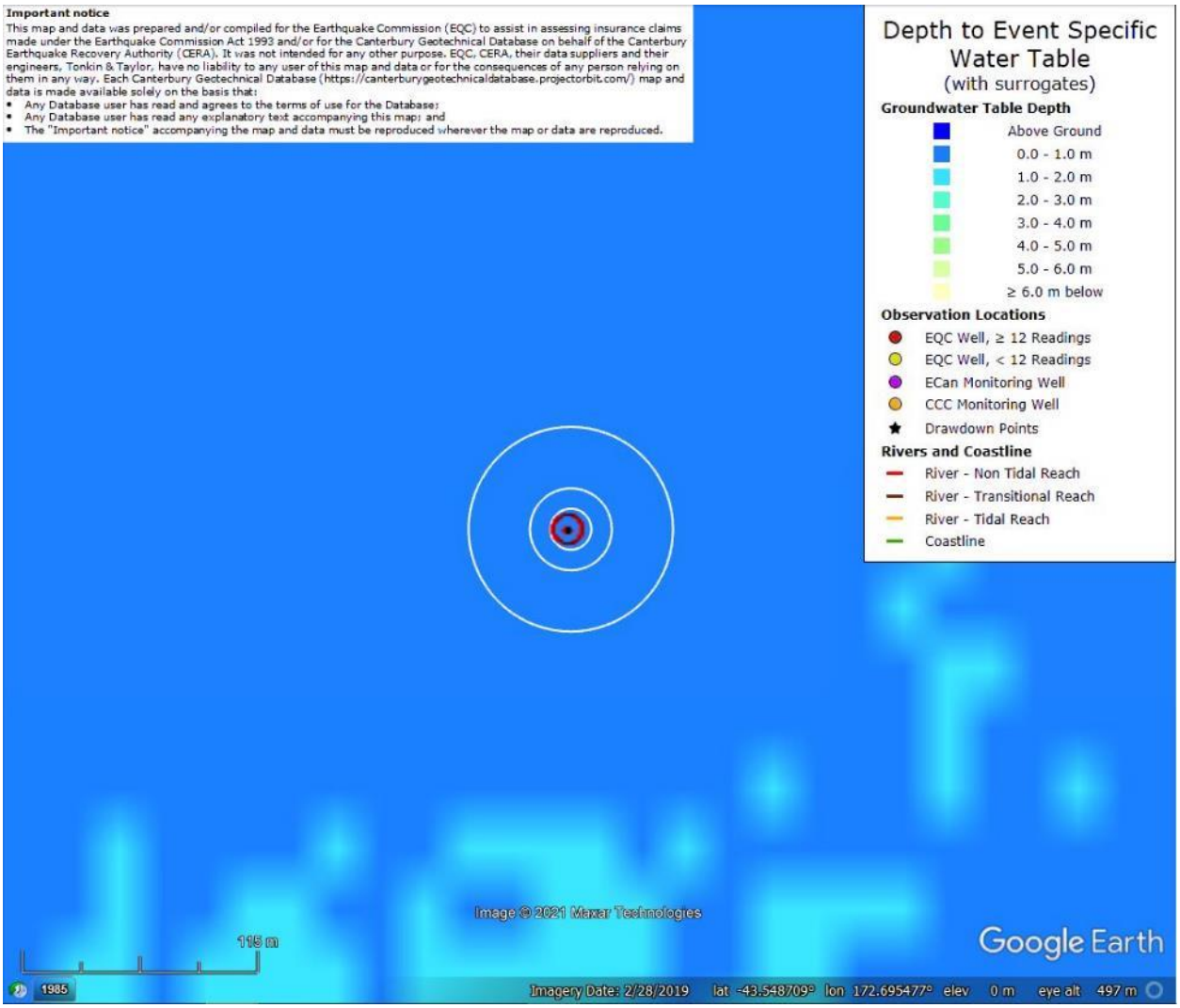

Figure 53: Depth to groundwater table for Feb-11 EQ.

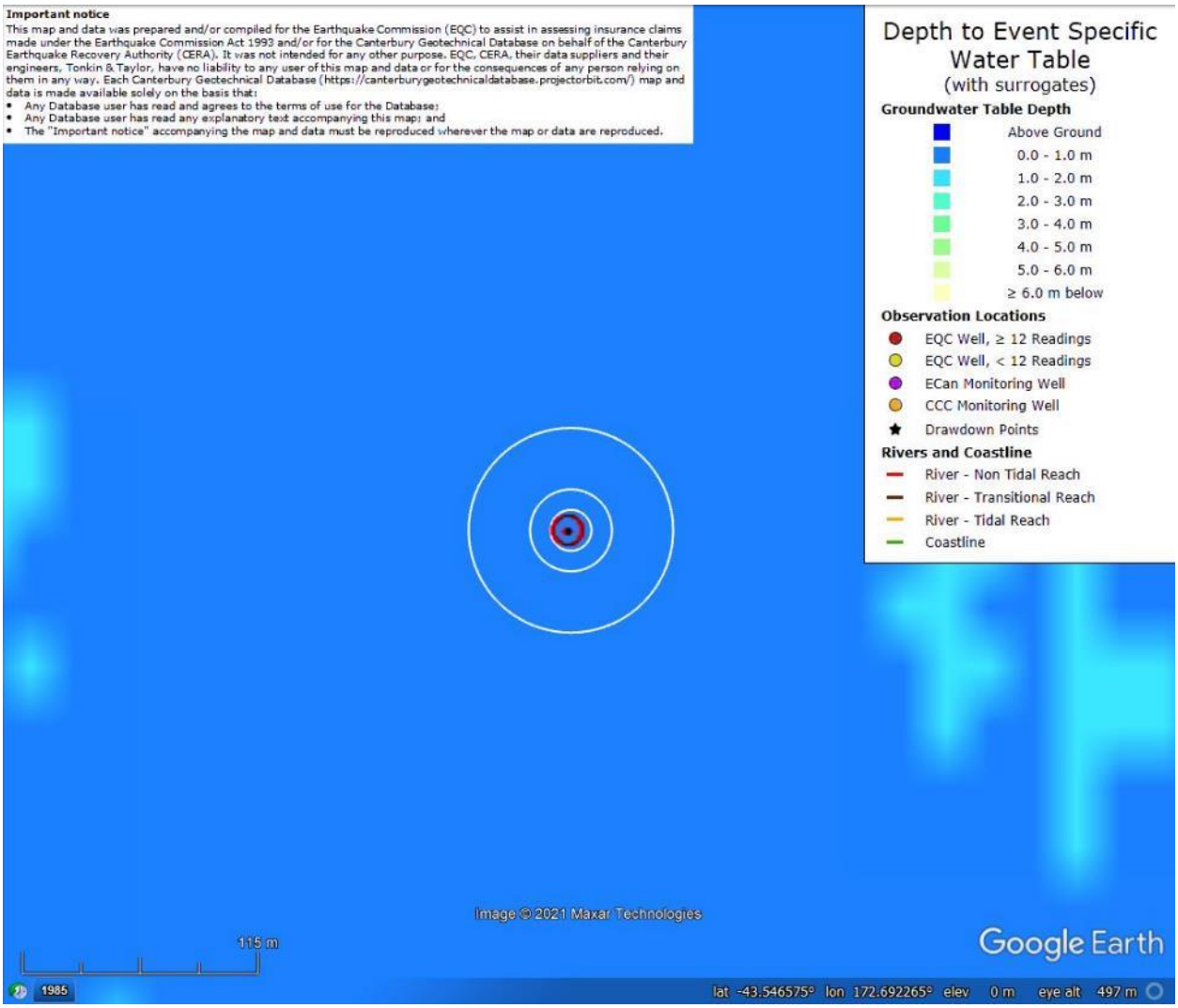

Figure 54: Depth to groundwater table for Jun-11 EQ.

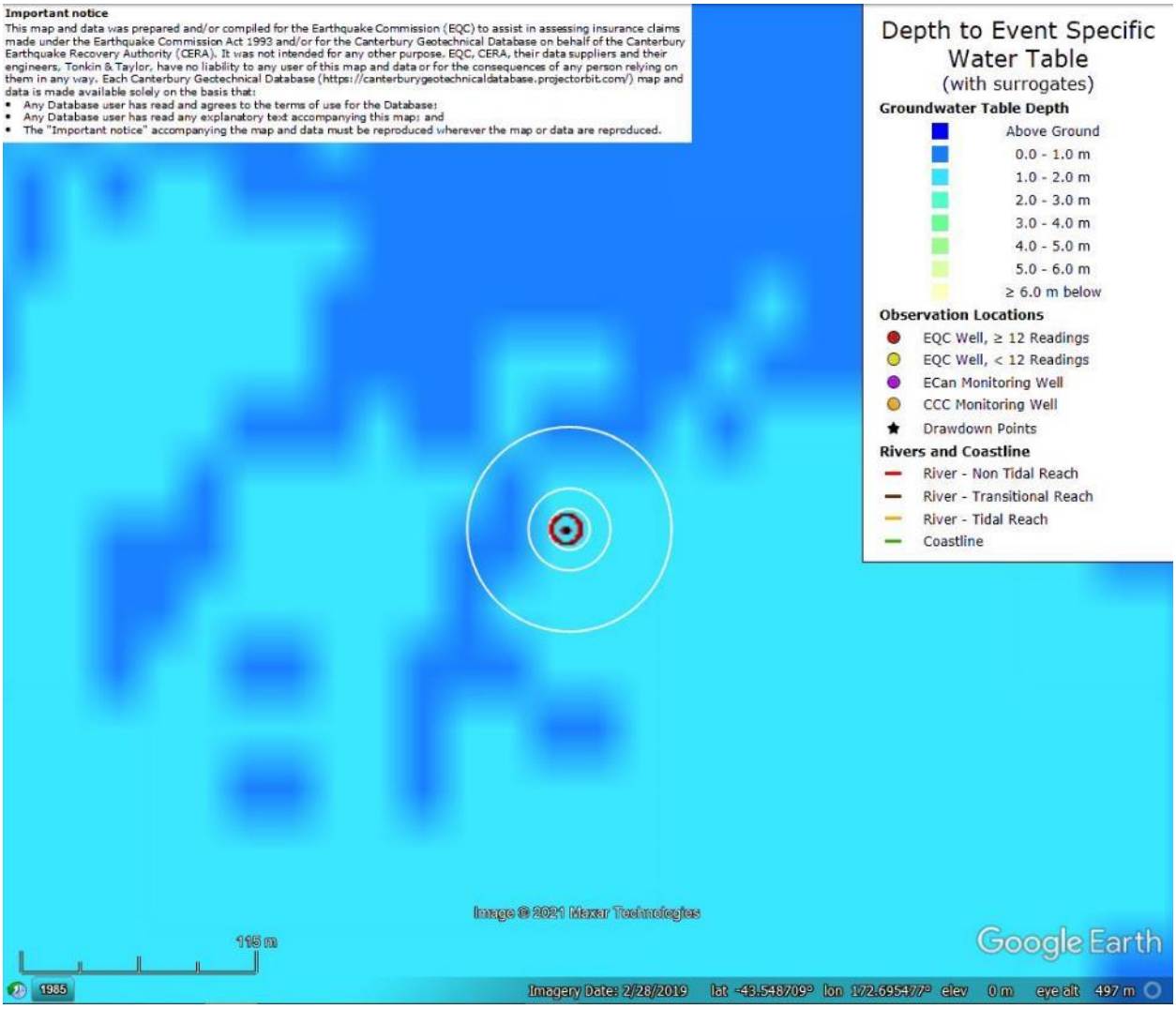

Figure 55: Depth to groundwater table for Dec-11 EQ.

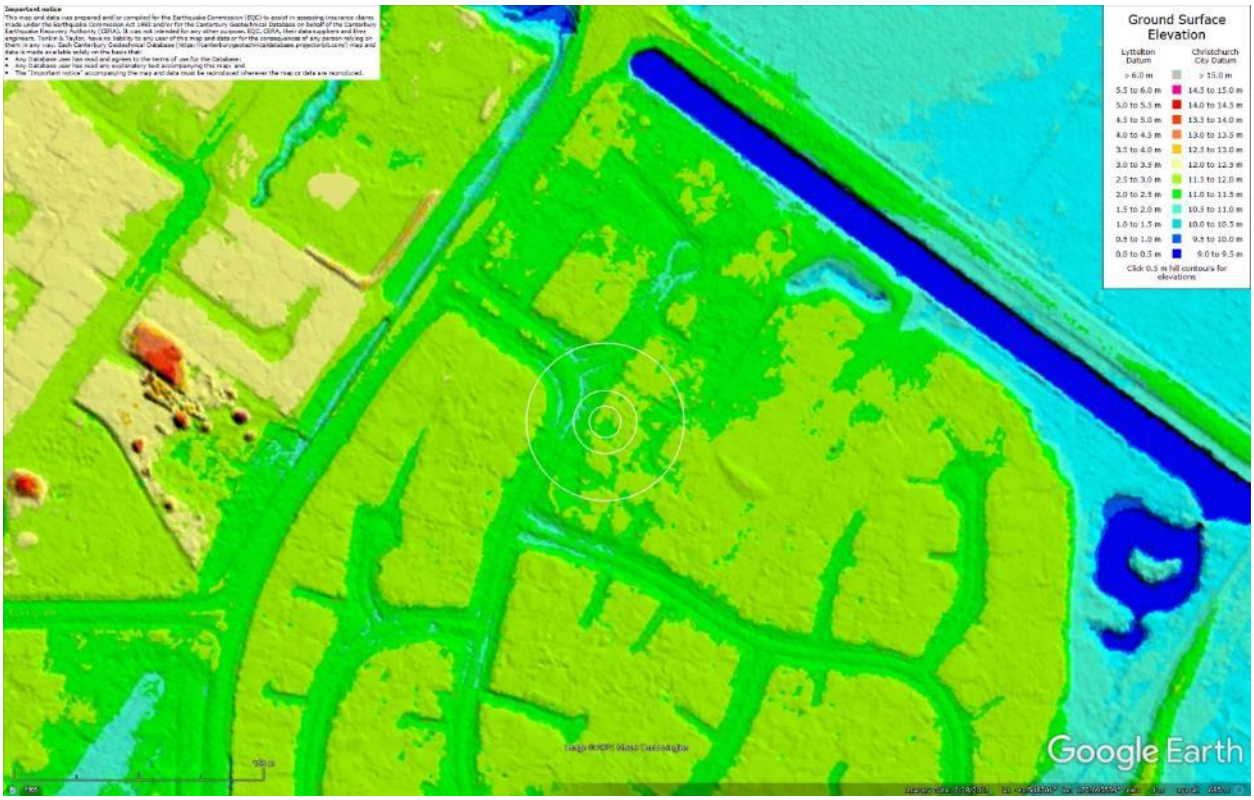

Figure 56: Ground surface elevation according to the Sep-11 LiDAR survey.

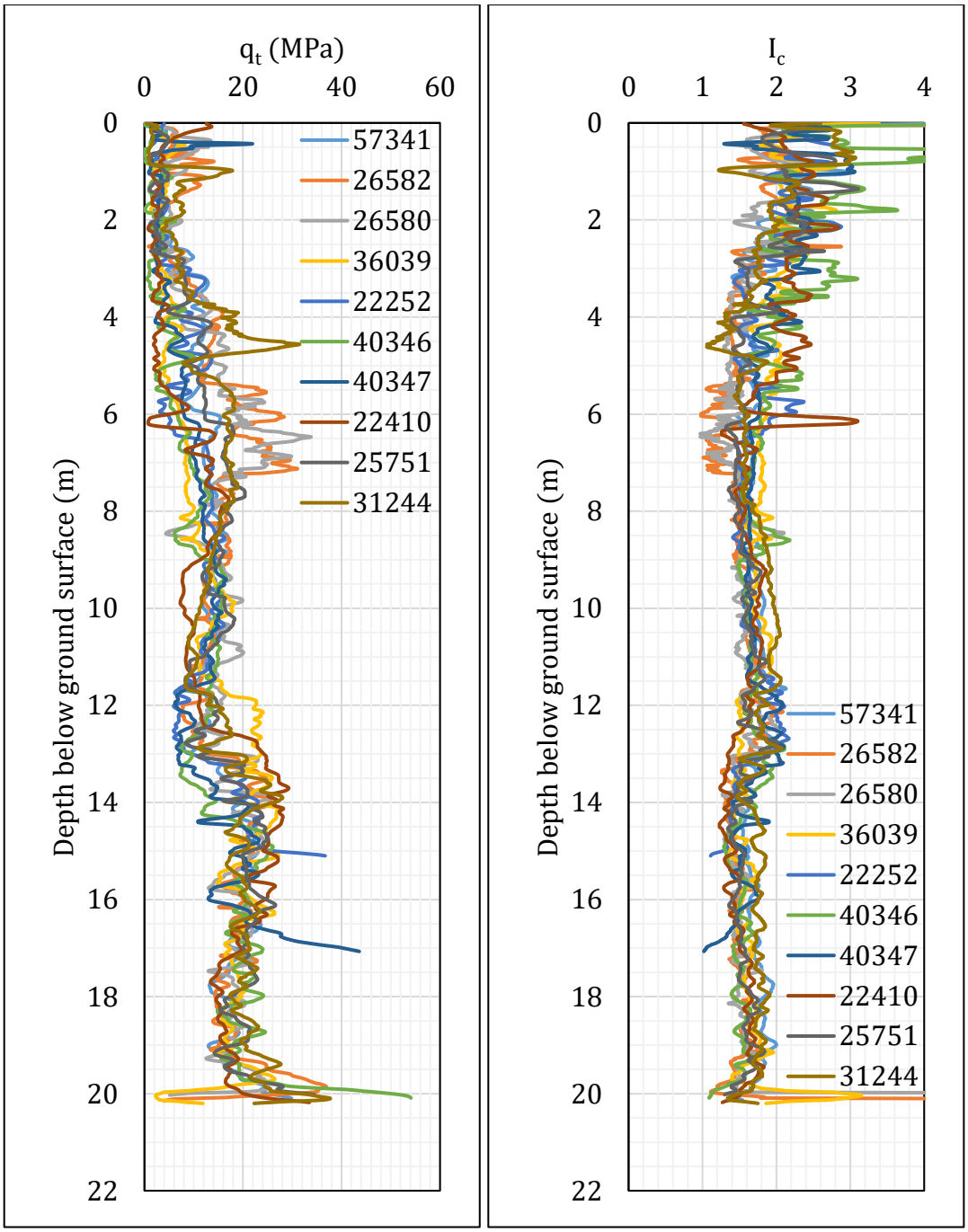

Figure 57: q_t and I_c profiles.

Note 6: The selection of CPTs for the area considered for settlement assessment (Figure 1) is based on the proximity of the CPTs to the considered areas. In accordance with that, the following table shows CPTs that were used for the volumetric settlement analysis in *Cliq v.3.0.3.2*, a CPT soil liquefaction software developed by GeoLogismiki. (The average volumetric settlements were reported in Table 8.)

Table 12: CPT profiles used in volumetric settlement analysis for areas selected for settlement assessment.

CPT ID No.	Patch A (10-m buffer)	Patch A (20-m buffer)	Patch A (50-m buffer)	Road (50-m buffer)
57341 (56581)	✓	✓	✓	✓
26582			✓	
26580			✓	
36039				✓
22252				
40346				
40347				
22410				✓
25751				✓
31244				

Table 13: CPT-based results.

		CPT ID							
EQ Event	Parameter	57341	26582	26580	36039	40346	22410	25751	31244
Sep-10	S_{V1D} (mm)	34	89	73	90	136	198	53	14
	LSN	14	16	22	23	25	43	16	5
	LPI	2	4	5	6	10	16	3	0
	LPI_{ish}	0	2	5	3	5	11	2	0
	$D_{FS<1}$ (m)	1.36	1.92	1.31	2.11	2.17	1.00	1.8	undet.
Feb-11	S_{V1D} (mm)	176	182	190	217	256	278	171	71
	LSN	50	32	42	52	42	66	46	17
	LPI	28	24	27	39	41	47	27	13
	LPI_{ish}	32	20	28	35	27	48	27	12
	$D_{FS<1}$ (m)	0.52	1.62	0.96	0.96	0.89	0.52	0.86	1.94
Jun-11	S_{V1D} (mm)	99	150	133	168	207	249	115	48
	LSN	35	26	34	44	35	59	36	14
	LPI	11	14	15	24	26	34	14	6
	LPI_{ish}	14	13	17	20	17	30	11	5
	$D_{FS<1}$ (m)	0.58	1.67	1.14	1.13	2.17	0.76	1.62	1.98
Dec-11	S_{V1D} (mm)	22	79	61	78	126	183	40	9
	LSN	8	13	18	18	22	37	11	3
	LPI	1	3	4	5	9	15	2	0
	LPI_{ish}	1	1	2	2	4	9	1	0
	$D_{FS<1}$ (m)	1.72	1.95	1.63	2.36	2.17	1.82	1.94	undet.

Notes: $D_{FS<1}$ = Depth to the first liquefiable layer ($FS_L<1$) that is at least 300-mm thick, as determined by the Boulanger and Idriss (2016) liquefaction-triggering procedure (P_L=50%, C_{FC}=0.13, and $I_{c,cutoff}$ =2.6), and exported from *Cliq v.3.0.3.2*; undet. = the specified soil layer was not detected.

Note 7: Based on the borehole log (BH 57236, Figure 1), the groundwater table is at a depth of 3.8 m below the ground surface. The soil profile consists of (1) topsoil (organic Silt, OL) to a depth of 0.25 m, (2) fine sand, SP, of the Christchurch formation to a depth of 0.8 m, (3) silt, ML, of the Christchurch formation to a depth of 3.25 m, and (4) fine to medium sand, SP, of the Christchurch formation to a depth of 15.65 m (the end of the borehole).

Note 8: The ejecta-induced free-field settlement provided in Table 11 is an areal average settlement due to ejecta, which is based on the total settlement assessment area, A_T (provided in Table 9 and repeated in Table 14). However, the considered area was not always covered completely with ejecta; thus, it is important to provide the localized ejecta-induced settlement, too. The localized settlement due to ejecta is estimated using photographic evidence only as

$$S_{E,P\_localized} = \frac{V_E}{A_E}$$

where V_E is the total volume of ejecta within A_T and A_E is the total coverage area of ejecta within A_T. Please note that the areal ejecta-induced settlement provided in Table 14 as S_{E,P_areal} is the same as $S_{E,P}$ in Table 11, which was estimated as

$$S_{E,P\_areal} = S_{E,P} = \frac{V_E}{A_T}$$

where V_E is the total volume of ejecta within A_T and A_T is the total settlement assessment area.

Table 14a: Areal and localized ejecta-induced settlement estimates for Patch A (10-m buffer) based on photographic evidence.

Earthquake Event	A_T (m^2)	A_E (m^2)	V_E (m^3)	S_{E,P_areal} (mm)	$S_{E,P\_localized}$ (mm)
Sep-10	306	0	0	0	0
Feb-11	306	64.4	5.6-10.1	25±5	120±35
Jun-11	306	70.5	3.5-7.1	20±5	75±25
Dec-11	306	6.0	0.1-0.2	<5	30±10

Notes: $S_{E,P\_areal} = S_{E,P}$ reported in Table 11 = areal ejecta-induced settlement; $S_{E,P\_localized}$ = localized ejecta-induced settlement; A_T = total settlement assessment area; V_E = total volume of ejecta within A_T; A_E = total area of ejecta within A_T; The estimates of both areal and localized ejecta-induced settlement are rounded to the nearest 5 mm; Final plus/minus values are also rounded to the nearest 5 mm.

Table 14b: Areal and localized ejecta-induced settlement estimates for Patch A (20-m buffer) based on photographic evidence.

Earthquake Event	A_T (m^2)	A_E (m^2)	V_E (m^3)	S_{E,P_areal} (mm)	$S_{E,P\_localized}$ (mm)
Sep-10	642	0	0	0	0
Feb-11	642	137	8.4-16.2	20±5	90±30
Jun-11	642	112	5.1-10.2	10±5	70±25
Dec-11	642	24.1	0.3-0.8	<5	25±10

Notes: S_{E,P_areal} = $S_{E,P}$ reported in Table 11 = areal ejecta-induced settlement; $S_{E,P\_localized}$ = localized ejecta-induced settlement; A_T = total settlement assessment area; V_E = total volume of ejecta within A_T; A_E = total area of ejecta within A_T; The estimates of both areal and localized ejecta-induced settlement are rounded to the nearest 5 mm; Final plus/minus values are also rounded to the nearest 5 mm.

Table 14c: Areal and localized ejecta-induced settlement estimates for Patch A (50-m buffer) based on photographic evidence.

Earthquake Event	A_T (m^2)	A_E (m^2)	V_E (m^3)	S_{E,P_areal} (mm)	$S_{E,P\_localized}$ (mm)
Sep-10	913	0	0	0	0
Feb-11	913	261	14.5-28.4	25±5	85±25
Jun-11	913	195	9.2-18.4	15±5	70±25
Dec-11	913	55.2	0.9-2.0	<5	25±10

Notes: S_{E,P_areal} = $S_{E,P}$ reported in Table 11 = areal ejecta-induced settlement; $S_{E,P\_localized}$ = localized ejecta-induced settlement; A_T = total settlement assessment area; V_E = total volume of ejecta within A_T; A_E = total area of ejecta within A_T; The estimates of both areal and localized ejecta-induced settlement are rounded to the nearest 5 mm; Final plus/minus values are also rounded to the nearest 5 mm.

Table 14d: Areal and localized ejecta-induced settlement estimates for Road (50-m buffer) based on photographic evidence.

Earthquake Event	A_T (m^2)	A_E (m^2)	V_E (m^3)	S_{E,P_areal} (mm)	$S_{E,P\_localized}$ (mm)
Sep-10	914	0	0	0	0
Feb-11	914	914	77.8-103	100±15	100±15
Jun-11	914	914	67.7-84.9	85±10	85±10
Dec-11	914	334	3.9-7.0	5±5	15±5

Notes: S_{E,P_areal} = $S_{E,P}$ reported in Table 11 = areal ejecta-induced settlement; $S_{E,P\_localized}$ = localized ejecta-induced settlement; A_T = total settlement assessment area; V_E = total volume of ejecta within A_T; A_E = total area of ejecta within A_T; The estimates of both areal and localized ejecta-induced settlement are rounded to the nearest 5 mm; Final plus/minus values are also rounded to the nearest 5 mm.

Summary 2:

- **The best estimate of the localized ejecta-induced free-field ground settlement at the Ti Rakau Reserve site for the SEP 2010, FEB 2011, JUN 2011, and DEC 2011 earthquake is 0 mm, 120±35 mm, 75±25 mm, and 30±10 mm, respectively.**
- **The best estimate of the localized ejecta-induced settlement of the road at the Ti Rakau Reserve site for the SEP 2010, FEB 2011, JUN 2011, and DEC 2011 earthquake is 0 mm, 100±15 mm, 85±10 mm, and 15±5 mm, respectively.**